AD-A063 311 AIRESEARCH MFG CO OF CALIFORNIA TORRANCE F/G 7/2
HIGH TEMPERATURE SLOW CRACK GROWTH IN SILICON CARBIDE.(U)
DEC 78 D E SCHWAB, D M KOTCHICK N00014-76-C-0249
UNCLASSIFIED 78-15574 NL

END
DATE FILMED
3-79
DDC

LEVEL II

(12)

AIRESEARCH MANUFACTURING COMPANY
OF CALIFORNIA

ANNUAL SUMMARY REPORT

HIGH TEMPERATURE SLOW CRACK GROWTH IN SILICON CARBIDE

(13 Oct 1976-13 Oct 1977)

78-15574

December 18, 1978

Research sponsored by

Office of Naval Research
Department of the Navy

Under Contract N00014-76-C-0249

AIRESEARCH MANUFACTURING COMPANY
OF CALIFORNIA

(9) ANNUAL SUMMARY REPORT. 13 Oct 76-13 Oct 77,

(6) HIGH TEMPERATURE SLOW CRACK GROWTH IN SILICON CARBIDE.
([redacted]77)

(14) 78-15574 (11) 18 Dec[redacted]78

(10) Prepared by
David [redacted] E. Schwab
[redacted]
and
David [redacted] M. Kotchick
Materials Engineering

(12) 57p.

for
Office of Naval Research
Department of the Navy

Under Contract (15) N[redacted]14-76-C-[redacted]0249

387 343

Approved: W. S. Miller
W. S. Miller
Program Manager

Approved: W. J. O'Reilly
W. J. O'Reilly
Chief Engineer
Heat Transfer and Cryogenic Systems

387 343

ACKNOWLEDGMENTS

This report was prepared by David E. Schwab, the Principal Investigator, and David M. Kotchick of the Materials Engineering Department. William S. Miller, of the Heat Transfer and Cryogenic Systems Department, served as Program Manager. The high-temperature testing was conducted at AiResearch by P. Patterson.

Mr. M. Keith Ellingsworth of the Power Program, Material Sciences Division, Office of Naval Research, was the Technical Monitor on the program. His guidance and support have been deeply appreciated.

Portions of this report have been submitted for publication to the Bulletin of the American Ceramic Society.

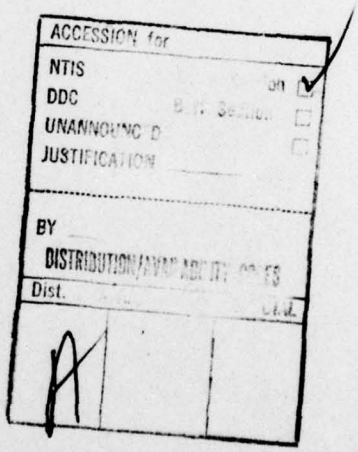

NOMENCLATURE

L	Load
m	Weibull modulus
n	Slow crack growth exponent
P_f	Failure probability
S	Stress
SASC	Trade name (sintered alpha silicon carbide)
SCG	Slow crack growth
SEM	Scanning electron microscope
SiC	Silicon carbide
V	Crack velocity or growth rate

CONTENTS

SECTION 1

INTRODUCTION

Silicon carbide is a candidate structural material for heat exchangers, turbines and other intricately-shaped devices that must operate at 1000 to 1700°C (1830 to 3090°F) in oxidizing and marine (salt-bearing) atmospheres. Its high strength and hardness at elevated temperatures, low density and thermal expansion, high thermal conductivity, oxidation and corrosion resistance and abundance of raw materials account for its candidacy for these applications. Problems of brittleness, variability of properties and high cost of manufacture remain, but are common to other contending materials as well. Of the available dense grades of SiC, only sintered α-SiC (SASC) is easily shaped and contains no low-melting free Si phase that would limit its use to 1340°C (2450°F). Lack of free Si also provides improved corrosion resistance[3,23].

The purpose of this investigation was to identify by survey the probable maximum use temperatures and stress levels for Sintered Alpha Silicon Carbide in expected marine (salt containing) and oxidizing environments as a function of sample surface condition. The results of this survey should be useful to define the areas where more detailed and more statistically significant experiments could be conducted.

SECTION 2

BACKGROUND

Perhaps because of much published research on environmental damage in metals over the past several years (e.g. hydrogen embrittlement, stress-corrosion, hot-salt corrosion, sulfidation and stress-alloying), there has been some concern that ceramics such as SiC may be vulnerable also. The chief concern has been a decrease in strength over long exposure times due to environmentally enhanced slow crack growth (SCG) and/or hot corrosion damage.

Small crack-like flaws cause fracture of SiC. Thus, corrosion pits, shallow intergranular attack or surface chemistry changes may be highly damaging if critical-size flaws are produced. On the other hand, surface-flaw healing or blunting and favorable surface chemistry changes may improve strength noticeably. Research to date has confirmed these expectations.

SLOW CRACK GROWTH (SCG)

SCG has been observed in silicon carbide. SiC compositions containing free silicon were tested from 20°C to 1500°C [14,10,11,12]*. Double-torsion tests[10,11] of three grades showed discontinuous crack growth during static loading and relatively high rates of crack growth under cyclic loading conditions. SCG in water at room temperature was observed and used in precracking the test specimens.

Another investigator[14] found that flexure strength increased at lower strain rates. This is the reverse of the expected behavior. Plasticity of the silicon-rich surface was believed to have accounted for the strengthening. Still another grade of SiC-Si material was tested[12] at varying strain rates in flexure. Strength degradation, presumably by SCG, was most pronounced above 1300°C and was related to softening melting of the Si-phase. Cracks were found to be healed by melting and freezing of Si, restoring most of the strength loss due to intentionally-created cracks.

Hot pressed SiC containing Al_2O_3 is also prone to SCG[2,13,15] as revealed by double-torsion and flexure tests at room and elevated temperatures in argon with H_2O, O_2 or SO_2 additions, in water and in air. Low temperature crack growth is believed to be a moisture-related stress-corrosion process. At high tempertures, plastic flow of the softened grain boundary phase is the suspected SCG mechanism.

Three grades of sintered SiC, not limited by Si, Al_2O_3 or other additions, are currently available or under development. The oldest, a commercially-available recrystallized 80 to 90 percent dense grade, exhibited discontinuous SCG at elevated temperatures[2]. The relatively large grain size (100 to 200μm) is thought to have contributed to the discontinuous nature of crack propagation.

---

*See list of references in Section 7.

Two dense, fine-grained (<10μm), sintered SiC grades are under development - beta-phase SiC and an alpha-phase SiC. Only the latter is commercially available. SCG evaluations of the α-SiC have been reported[9,13,8]. Double-torsion tests revealed no SCG below 1500°C, except in water at room temperature with characteristics similar to hot-pressed SiC. At 1600°C, SCG was observed in flexure tests at varying stess rates, but the secondary phenomenon of oxidation-contamination damage in a Pt-Rh element air furnace[8] interfered with quantitative SCG measurements.

OXIDATION/CORROSION RESISTANCE

Despite thermodynamic predictions of instability in molten salts and slags, SiC is highly resistant to attack in most important environments, including slags formed from coal fly ash[3,11]. Hot-pressed SiC and porous recrystallized SiC were severely attacked when immersed in 1000°C molten Na_2SO_4[1]. However, limited tests of hot-pressed SiC exposed to 1100°C combustion gases containing lower concentrations of salt (Na, V, Mg and S) revealed no apparent strength degradation[16]. In fact, exposure to 1400°C air healed thermal-shock cracks in 80 percent dense SiC flexure specimens, doubling the strength[7]. Similarly, flexure strength increases of 10 to 15 percent have been reported for machined sintered bars of α-SiC exposed to 50 thermal cycles in 1070°C combustion gases[17], and for β-SiC exposed for 10 to 1000 hours in 1500°C air[8] or 20 minutes in 0.35 torr He at 1650 to 1950°C[18]. The latter exposure was shown to produce rounding of crack tips as the surface layers of SiC dissociated to form Si(g) and C(s).

LIFE PREDICTION

The design life of a ceramic component depends upon the stresses to which it is subjected and the acceptable probability of failure (risk). The mathematical relationships linking strength, probability and time have been under development for some time and have been applied to practical ceramic products including grinding wheels[20], spacecraft windows,[21,22] gas turbine components and heat exchangers[19]. To employ these relationships, knowledge of the properties of the ceramic in the expected environment is required. In particular, the initial distribution of flaws throughout the material, and the stress-dependence of the subcritical crack growth rate must be known.

Of the various experimental methods of obtaining this information, variable stress-rate flexure tests of bars[4] is perhaps the most direct for two reasons. First, it permits natural, microscopic flaw distributions (e.g., as-fired, machined or environmentally exposed) to be characterized by means of relatively simple, inexpensive flexure tests of small bars. Second, it directly measures the strength-degrading effects of the flaws. Double-torsion tests, on the other hand, measure the growth of a large, artificial crack and provide no statistical strength data.

SECTION 3

EXPERIMENTAL PROCEDURE

MATERIALS

Billets of sintered -SiC (SASC)* were prepared by cold-pressing and sintering. Flexure bars were each 2.5 x 5 x 44 mm. Each of the specimens was cut from the top surface of SASC billets, leaving the top face as-formed and as-fired. The bottom face of each sample was ground transversely with 200-grit diamond and then finished with 400-grit diamond. Long edges were lightly chamfered by hand with 220-grit diamond lapping compound. Width and thickness were within 0.13 mm of specified values. Ground surfaces were flat within 25μm. Ground sides were parallel within 25 μm and were perpendicular to the faces within 1 deg. Visual, fluorescent dye-penetrant and radiographic inspections ensured that each specimen was free of defects greater than 0.5 mm long.

Density, measured by the immersion method**, varied from 3.07 to 3.16 g/cc. Metalographic analysis revealed equiaxed grains averaging 8.6 μm in diameter. The microstructure is shown in Figure 1.

For each test, specimens were selected at random from among the various billets, so that the usual batch-to-batch property variations due to composition and processing differences would influence all the test groups in the same way. Most specimens were tested on the as-fired face because most surfaces of formed parts are expected to remain as-fired. A few test groups were tested on the machined face to simulate cut and ground surfaces as well. The surfaces of certain specimens were wiped with isopropanol and were subsequently treated to permit corrosion and oxidation effects to be evaluated. Some were oxidized by heating 65h in air at 1260°C; others were coated with concentrated artifical ocean saltwater***, heated at 120°C to evaporate the water and then subjected to 65h at 900°C plus 16h at 1260°C in air in an electric furnace. The surface to be tested (as-fired or ground) faced upward during the oxidation or salt treatment so that the oxidation or corrosion process would be uniform. The samples were cooled slowly in the furnace.

FLEXURE TESTING

Flexure tests were conducted in a SASC floating-pin, 4-point bend fixture* having a 38mm outer span and a 13mm inner span. Loads were applied by a universal test machine (Instrom Corp.) at varying speeds, through silicon carbide push rods. Loading rates, recorded autographically, were converted to strain rates through the equation

$$\dot{\epsilon} = \frac{1.5\,\dot{L}}{WH^2E} \qquad (1)$$

---

*Carborundum Co.
**ASTM-C373-72
***ASTM-D1141-52 (without heavy metals)

500 X

F-28107

Figure 1. Sintered Alpha SiC Microstructure

where L is the recorded load rate, W is the specimen width, H is the specimen thickness and E is the Young's modulus. A value of 414 GPa (60 Mpsi) was used for E at all temperatures, based upon available data[5,6].

The fixture and specimen were contained within a silicon carbide element electric furnace which provided temperatures as high as 1620°C. Temperatures were monitored with a micro-optical pyrometer and were within 3°C of the reported value.

Fracture surfaces of each specimen were examined under low-magnification steromicroscopes to locate the fracture origin. Selected specimens were examined by scanning electron microscopy (SEM).

SECTION 4

RESULTS

The results of each group of replicate tests were plotted in Weibull form, as shown in Figure 2. The computed arithmetic mean strength, standard deviation, median strength (at 50 percent failure probability) and Weibull modulus (m) are shown. A least-squares straight line fit was used to compute m, as defined by the linear equation

$$\ln \ln\left[1/(1-P_f)\right] = m \ln S + \ln S_o \qquad (2)$$

where P_f is the failure probability, S is stress and S_o is a constant. The results are summarized in Table 1 for all groups of specimens. Detailed data are shown in Appendix A.

Various strain rates were used to test groups of samples at a given surface condition and temperature. Results of these tests were plotted on a logarithmic scale as strength versus strain rate. The mean strength and strain rate for each group of data were fit to a straight line (Figure 3) to obtain the slow crack growth exponent (n) defined by

$$V = AK^n \qquad (3)$$

and

$$\left(S_1/S_2\right)^{n+1} = \dot{\varepsilon}_1/\dot{\varepsilon}_2 \qquad (4)$$

where V is the crack growth rate, A is a constant, K is the stress intensity factor, and S_1 and S_2 are the strengths of samples tested at strain rates $\dot{\varepsilon}_1$ and $\dot{\varepsilon}_2$, respectively.

Figure 4 shows typical surface and subsurface pores at fracture orgins. Note the angular, sharp appearance of grains in the pore of the as-fired sample (a), compared with the rounded appearance of grains in the oxidized pore (b). In (c) the porous origin has a relatively flat shape and angular grains. Table II summarizes the results of SEM analysis of fracture origins.

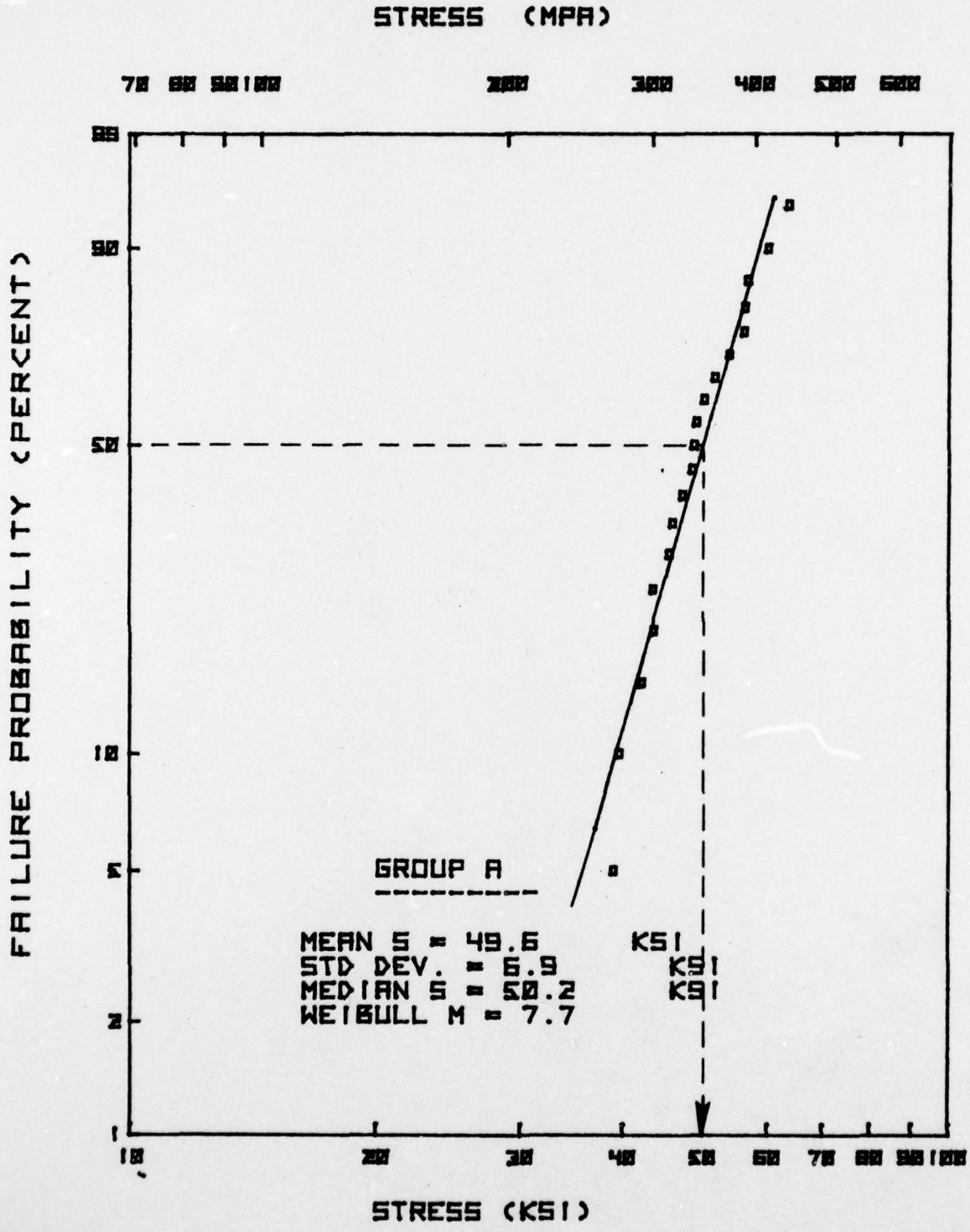

Figure 2. Weibull Plot

TABLE 1

FLEXURE TEST RESULTS

Group	Surface Condition	Temp. (C)	$\dot{\epsilon}$ (10^{-6}/sec)*	Strength (ksi)			Weibull Constant		No. of Tests
				Mean	Std. Dev.	Median#	m	n	
A	As-fired	20	50	49.6	6.9	50.2	7.7		19
F		1060	2	56.9	6.1	57.3	8.0		5
H		1340	50	54.9	5.7	55.3	8.2	29.9	5
I			3	50.5	5.9	50.9	7.6		6
P		1620	60	33.9	3.6	34.2	8.2	14.7	6
Q			1	26.6	2.7	26.8	9.1		6
BB	As-fired	20	50	58.5	7.0	59.0	8.0		9
JA	Plus oxidized	1340	40	53.2	6.4	53.7	7.5	27.0	8
WB			1	46.6	5.7	47.1	7.8		9
35		1620	30	30.9	5.2	31.0	-		4
C	As-fired	20	50	54.1	7.7	54.6	6.8		10
G	Plus salted	1060	5	53.6	4.4	53.9	10.1		5
K		1340	50	56.6	5.8	57.1	9.4	11.9	9
L			6	51.7	8.5	52.2	5.2		6
M			2	44.0	5.6	44.4	7.4		9
R		1620	30	33.0	3.0	33.2	10.1	16.5	6
S			2	26.6	-	-	-		1
T			0.5	26.3	4.4	26.5	4.8		5
D	Ground$^{\Delta}$	20	90	50.7	3.4	51.0	13.7		7
N		1340	90	55.6	6.2	56.1	7.4		5
X		1620	1	27.9	-	27.9	-		1
V	Ground$^{\Delta}$ Plus salt	20	90	52.2	-	52.2	-		1
E			3	49.3	9.7	49.7	4.5		8
Y		1340	40	52.2	8.4	52.6	5.3	38.4	5
O			2	48.4	8.6	48.9	5.4		10
Z		1620	30	36.3	5.6	36.6	5.7	8.3	5
U			0.5	23.1	2.0	23.2	9.5		5

*Average of actual values #Weibull curve intercept at $P_f = 0.5$ $^{\Delta}$Transverse to long axis

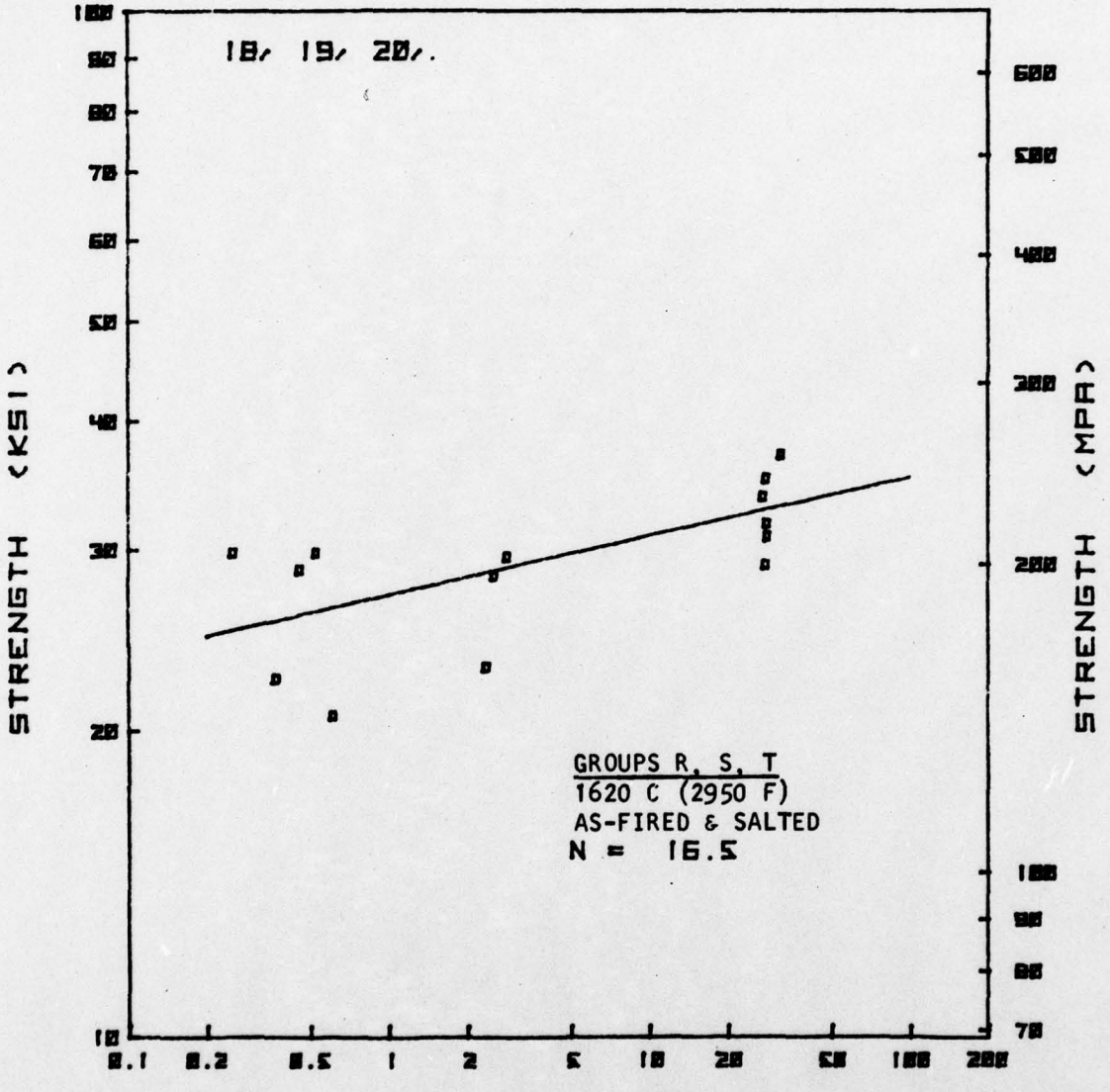

Figure 3. Strength-Strain Rate Plot

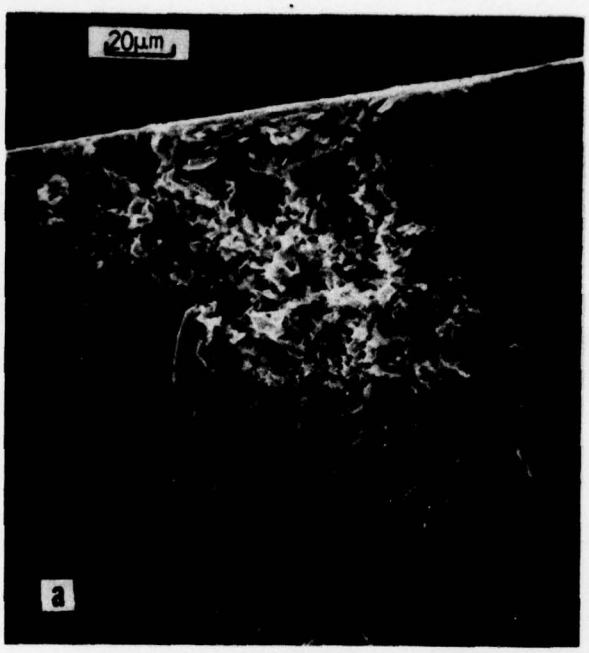

(a) Surface pore, as-fired Group A sample

(b) Surface pore, oxidized as-fired Group B sample

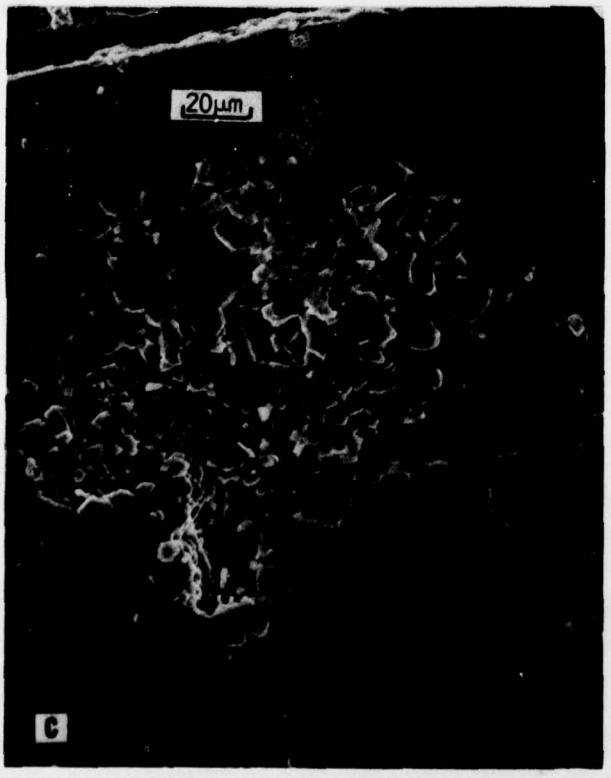

(c) Subsurface pore, salt-coated as-fired Group M sample

F-29007

Figure 4. Scanning-Electron Micrographs of SASC Fracture Origins

TABLE II

FRACTURE ORIGINS

Group	Surface Condition	Temp. (C)	Strength	Surface Defect				Subsurface Pore	Unknown
				Pore	Large Grain	Other	Total		
A	As-fired (Fast Straining)	20	High	-	-	2	2	1	-
			Low	1	-	3	4	1	1
			Total	1	-	5	6	2	1
BB	As-fired plus oxidized (Fast Straining)	20	High	-	-	-	-	2	-
			Low	1	1	-	2	1	-
			Total	1	1	-	2	3	-
K	As-fired plus salted (Fast straining)	1340	High	-	-	2	2	-	-
			Low	-	-	2	2	1	-
			Total	-	-	4	4	1	-
M	As-fired plus salted (Slow straining)	1340	High	-	-	1	1	-	-
			Low	-	-	-	-	3	-
			Total		-	1	1	3	-

SECTION 5

DISCUSSION

Effect of Temperature, Surface Condition and Strain Rate Upon Strength

When rapidly strained (30 to 90/Msec), SASC exhibited a small increase in strength (except oxidized samples) from 20 to 1340°C, and a marked decrease in strength at 1620°C (Figure 5). Slow straining (0.5 to 6/Msec) produced a small strength decrease from 1060 to 1340°C and a larger strength decrease from 1340 to 1620°C than rapid straining produced (Figure 6).

The 18 percent increase in 20°C mean strength (Figure 7) achieved by oxidation pretreatment is in good agreement with previous findings[7,8,17]. At 20°C, whereas 3 of 4 as-fired (A) samples failed from surface defects, only 4 of 10 oxidized (BB) samples did so (Table II). Admittedly the fractographic sample is small, but it appears likely from these results that oxidation did heal some surface defects. Indeed, Figure 4b shows rounding and smoothing of grains after oxidation.

The fracture strength of as-fired and salted samples tested at 1340°C tended to be limited by surface defects at high strain rates and by subsurface defects at slow strain rates (TableII). It is likely that slow straining proivdes time to heal surface flaws. However, the salt may be causing some subsurface defects by an undetermined mechanism. Clearly, more data are needed. Otherwise, the effect of surface condition and pre-exposure to hot salt or air was small, and within the scatter of the data for all test temperatures for which comparisons could be made (Figure 7 and 8). This is in agreement with trends of similar experiments on SiC materials by others[8,16,17].

LONG-TERM STRENGTH PREDICTION

The significance of the above data can be expressed by computing, for each test conditon, the estimated stress, S_e, that can be sustained for a given life, t_e, without failure at a designated probability level. To compute this stress, the SPT (strength-probability-time) relationships described by Davidge, et. al.[1] were combined mathematically to yield the following:

$$S_e = \frac{S_m(-\ln P_s)^{1/m}}{\left[(n+1)(t_e/t^*)\right]^{1/n}} \qquad (5)$$

where S is the median strength of samples tested under constant strain rate for a fracture time t^* and $P_s = 1-P_f$. For a given set of data, fracture time varies as the strength varies. It is reasonable and convenient to approximate $t^* = S_m/E$ for each data set. Thus,

$$S_e = \frac{S_m^{\frac{n+1}{n}}(-\ln P_s)^{1/m}}{\left[(n+1)(t_e E\dot{\epsilon})\right]^{1/n}} \qquad (6)$$

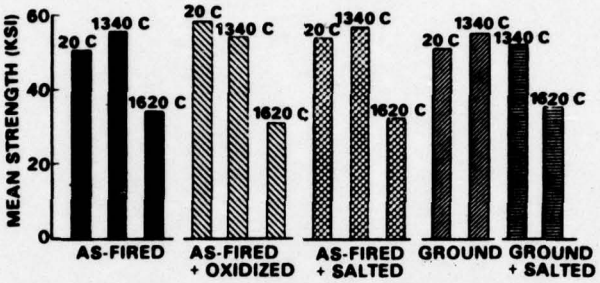

Figure 5. Effect of Temperature/Rapid Straining

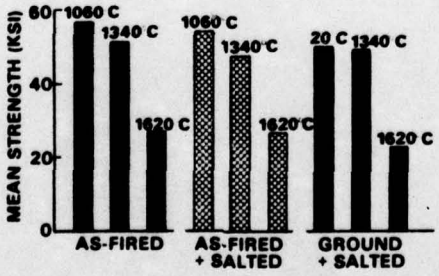

Figure 6. Effect of Temperature/Slow Straining

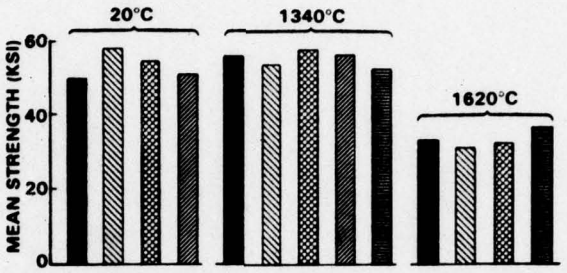

Figure 7. Effect of Surface Conditions/Rapid Straining

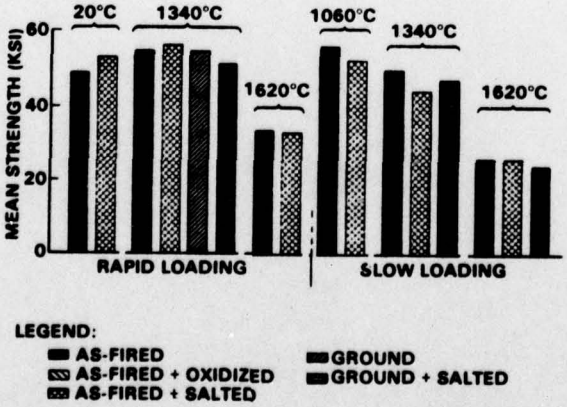

Figure 8. Effect of Salt/Rapid and Slow Straining

Equation (6) permits strengths to be computed rather quickly for any survival probability and lifetime of interest, provided that the material properties n, m and S_m at known t* are known. This may be much less tedious and more exact than constructing and interpreting SPT diagrams for each temperature/surface condition combination. Alternatively, the time to failure can be computed from a rearrangement of equation (5), yielding

$$t_e = \left(\frac{t^*}{n+1}\right) (-\ln P_s)^{n/m} (S_e/S_m)^n \qquad (7)$$

APPLICATION TO CERAMIC HEAT EXCHANGER DESIGN

The procedures discussed above allow calculation of design stresses for a given heat exchanger problem statement. As an example, taking $P_s = 0.999$ and a desired life of 500h (1.8 Msec,) the estimated strength is

$$S_e\ (500h,\ 0.999\ P_s) = \frac{S_m^{\frac{n+1}{n}} (0.001)^{1/m}}{\left[(n+1)(128\times10^9)\dot{\epsilon}\right]^{1/n}}$$

Table III compares predicted strengths for several of the surface conditions and temperatures tested. Figure 9 displays the results in graphical form.

A statistic worth mentioning is the lower variability in strength for as-received ground surfaces, compared with as-fired surfaces at 20°C. This result warns that the common practice of testing only ground surfaces at room temperature will often result in underestimating the variability of as-fired and elevated-temperature strengths. Clearly, the 500h strength of as-fired SASC at 1340°C and $P_s = 0.999$ is degraded significantly (52 percent) by salt exposure. Oxidation exposure without salt degraded the as-fired strength only 11 percent at the same temperature and reliability level. The strength of salted ground SASC was not as low as salted as-fired material.

At 1620°C, the 500h as-fired strength is not strongly degraded by salt exposure, but it is already at a relatively low level compared with 1340°C. However, ground plus salted samples had very low predicted strengths at 1620°C.

From a design standpoint, it is interesting to compare the 500h strengths of as-fired (unsalted) with ground and salted SASC at 1340°C and two reliability levels. For 50 percent probability of success, as-fired surfaces are about 3 percent weaker, but for 99.9 percent probability of success, as-fired surfaces are 44 percent stronger. This fact is a direct consequence of the difference in Weibull moduli for the two surface conditions.

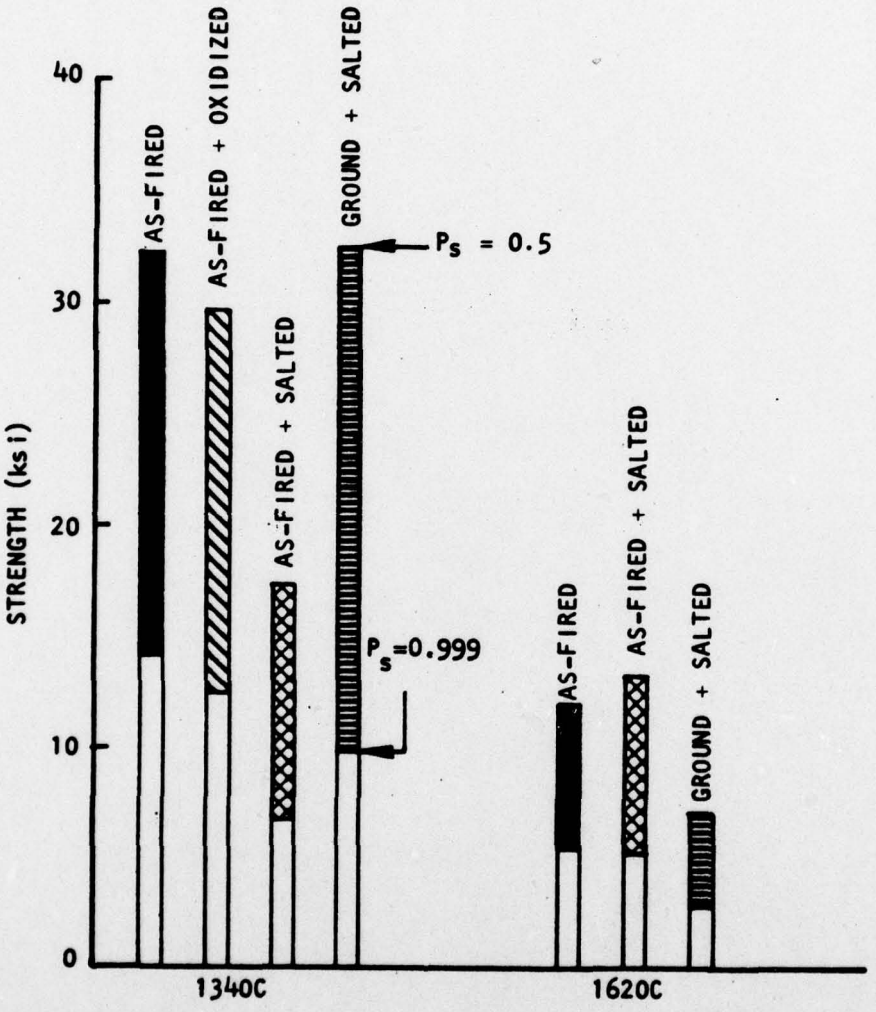

Figure 9. Predicted Strengths for SASC Bars for 500h Life

TABLE III

PREDICTED STRENGTHS FOR SASC BARS FOR 500h LIFE AT P_s = 0.999 AND 0.5

Surface Condition	Temperature (C)	S_e (Ksi)*	
		P_s = 0.999	P_s = 0.5
As-fired	1340	14.1	32.2
	1620	5.6	12.0
As-fired plus oxidized	1340	12.6	29.7
As-fired plus salted	1340	6.8	17.1
	1620	5.2	13.2
Ground plus salted	1340	9.8	33.3
	1620	2.8	6.7

*Average of values calculated at each of the strain rates tested.

SECTION 6

CONCLUSIONS

SASC suffers a large strength decrease from 1340 to 1620°C. From 20 to 1340°C there is little change in strength due to temperature, strain rate or surface condition with these exceptions:

(a) Ground surfaces show less strength variation at 20°C than as-fired surfaces.

(b) Preoxidation at 1260°C increases the 20°C mean strength of as-fired surfaces 18 percent. This seems to be related to rounding of surface defects during the preoxidation.

(c) At 1340°C, ocean-salt coating increased the strain-rate dependence of strength for as-fired samples. Reduced strength of these samples appears to be related to subsurface defects being the origins of the slow-strain failures, rather than the more common surface defect origins.

SECTION 7

REFERENCE

1. R. E. Tressler, M. D. Meiser and T. Yonushonis, "Molten Salt Corrosion of SiC and Si_3N_4 Ceramics," J. Amer. Ceram. Soc. 59 (5-6) 278-279 (1976).

2. K. D. McHenry and R. E. Tressler, "Subcritical Crack Growth in Silicon Carbide", J. Mater. Sci. 12 (1977) 1272-1278.

3. R. A. Perkins and H. W. Lavendal, "Reaction of Silicon Carbide with Fused Coal Ash", Final Report EPRI AF-294, Electric Power Research Institute, Palo Alto, CA 94304, November, 1976.

4. R. W. Davidge, J. R. McLaren and G. Tappin, "Strength-Probability-Time (SPT) Relationships in Ceramics," J. Mater. Sci. 8 (1973) 1966-1705.

5. E. H. Kraft and G. I. Dooher, "Mechanical Response of High-Performance Silicon Carbides," Presented at 2nd International Conference on Mechanical Behavior of Materials, Boston, MA, August, 1976.

6. D. C. Larsen and G. C. Walther, "Property Screening and Evaluation of Ceramic Vane Materials," Report No. IITRI-D6114-17R-24, IIT Research Institite, Chicago, IL, October 1977.

7. F. F. Lange, "Healing of Surface Cracks in SiC by Oxidation," J. Amer. Ceram. Soc. 53(5) 290 (1970).

8. C. A. Johnson and S. Prochazka, "Investigation of Ceramics for High Temperature Turbine Components," Report NADC-75228-30, Naval Air Development Center, Warminster, PA, June, 1977.

9. G. G. Trantina and C. A. Johnson, "Subcritical Crack Growth in Boron-Doped SiC," J. Amer. Ceram. Soc. 58 (7-8) 344-345 (1975).

10. D. E. Schwab and H. A. Warren, "High-Tempe ature Slow Crack Growth in Silicon Carbide," Report No. 77-13571, AiResearch Manufacturing Co. of California, Torrance, CA, March, 1977.

11. A. Pietsch, "Coal-Fired Prototype High-Temperature Continuous-Flow Heat Exchanger, "Report No. AF-684, Electric Power Research Institute, Palo Alto, CA, February 1978.

12. G. G. Trantina, "Fracture of a Self-Bonded Silicon Carbide," Ceramic Bulletin 57 (4)440-443 (1978).

13. A. G. Evans and F. F. Lange, "Crack Propagation and Fracture in Silicon Carbide," J. Mater. Sci. 10 (1975) 1659-64.

14. R. W. Davidge, G. Tappin and J. R. McLaren, "Strength Parameters Relevant to Engineering Applications for Reaction Bonded Silicon Nitride and REFEL Silicon Carbide," Powder Metall. Int., pp. 110-114, August, 1976.

15. K. D. McHenry, T. M. Yonushonis and R. E. Tressler, "Low Temperature Subcritical Crack Growth in SiC and Si_3N_4, J. Amer. Ceram. Soc. 59 (1976).

16. S. C. Singhal, "Corrosion-Resistant Structural Ceramic Materials for Gas Turbines," in Report No. MCIC-75-27, Battelle Memorial Institute, Columbus, Ohio, July 1974.

17. R. E. Wallace, "Ceramic Gas Turbine Engine Demonstration Program, Interim Report No. 4". Report No. 76-212188(4), AiResearch Mfg. Co. of Arizona, Phoenix, AZ, March 1977.

18. C. A. Johnson, "Crack Blunting in Sintered SiC," in Fracture Mechanics of Ceramics, Vol. 3. (ed. by R. C. Bradt, et. al.,) Plenum Press, New York, (1973)99-111.

19. M. Coombs and D. M. Kotchick, "High-Temperature Ceramic Heat Exchanger Development," Report No. 78-15251, AiReseach Mfg. Co. of California, Torrance, CA, June 1978.

20. J. E. Ritter Jr. and S. A. Wulf, "Evaluation of Proof Testing to Assure Against Delayed Failure," Ceramic Bulletin 57 (2) 186-192 (1978).

21. S. M. Wiederhorn, et. al., "A Fracture Mechanics Study of the Skylab Windows," pp. 829-42 in Fracture Mechanics of Ceramics, Vol. 2, ed. by R. C. Bradt, et. al., Plenum Press, New York (1974).

22. S. M. Wiederhorn, et. al., "Application of Fracture Mechanics to Space-Shuttle Windows," J. Amer. Ceram. Soc., 57, 319-23 (1974).

23. J. A. Costello and R. E. Tressler, personal communication.

APPENDIX A

TEST DATA

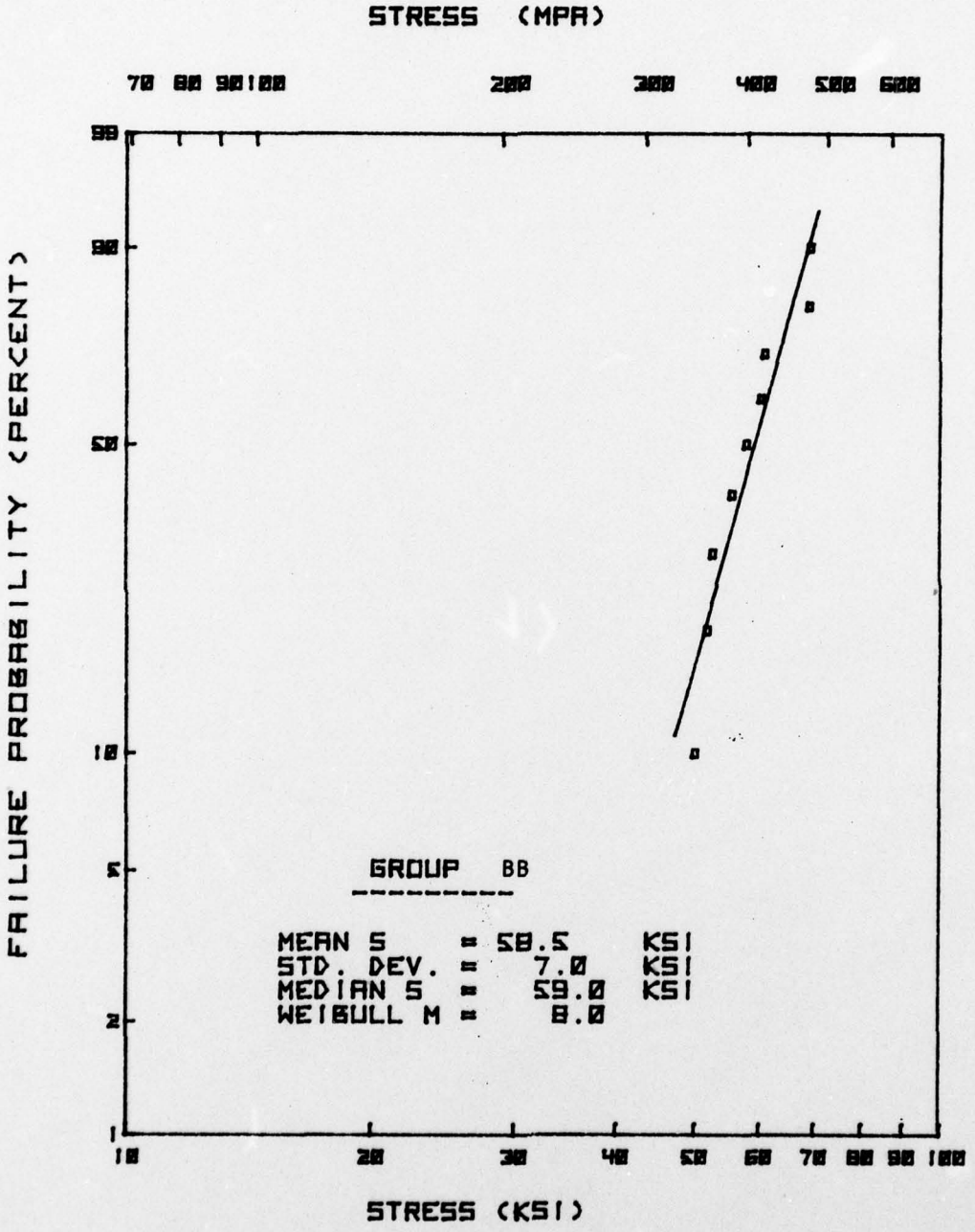
STRESS (MPA)
70 80 90 100 200 300 400 500 600
99
90
50
10
5
2
1
FAILURE PROBABILITY (PERCENT)
GROUP BB
MEAN S = 58.5 KSI
STD. DEV. = 7.0 KSI
MEDIAN S = 59.0 KSI
WEIBULL M = 8.0
10 20 30 40 50 60 70 80 90 100
STRESS (KSI)

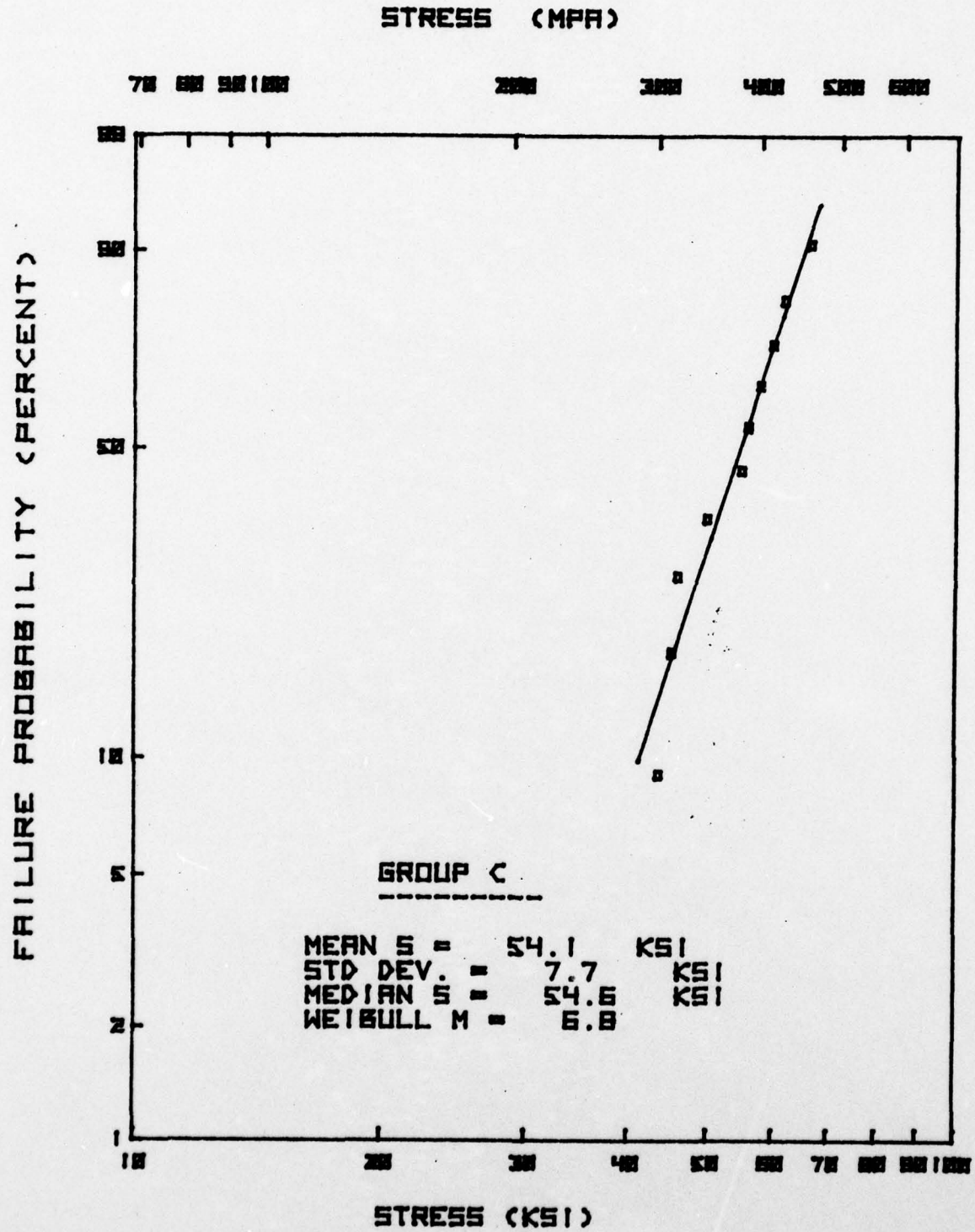
STRESS (MPA)
FAILURE PROBABILITY (PERCENT)
GROUP C
MEAN S = 54.1 KSI
STD DEV. = 7.7 KSI
MEDIAN S = 54.6 KSI
WEIBULL M = 6.8
STRESS (KSI)

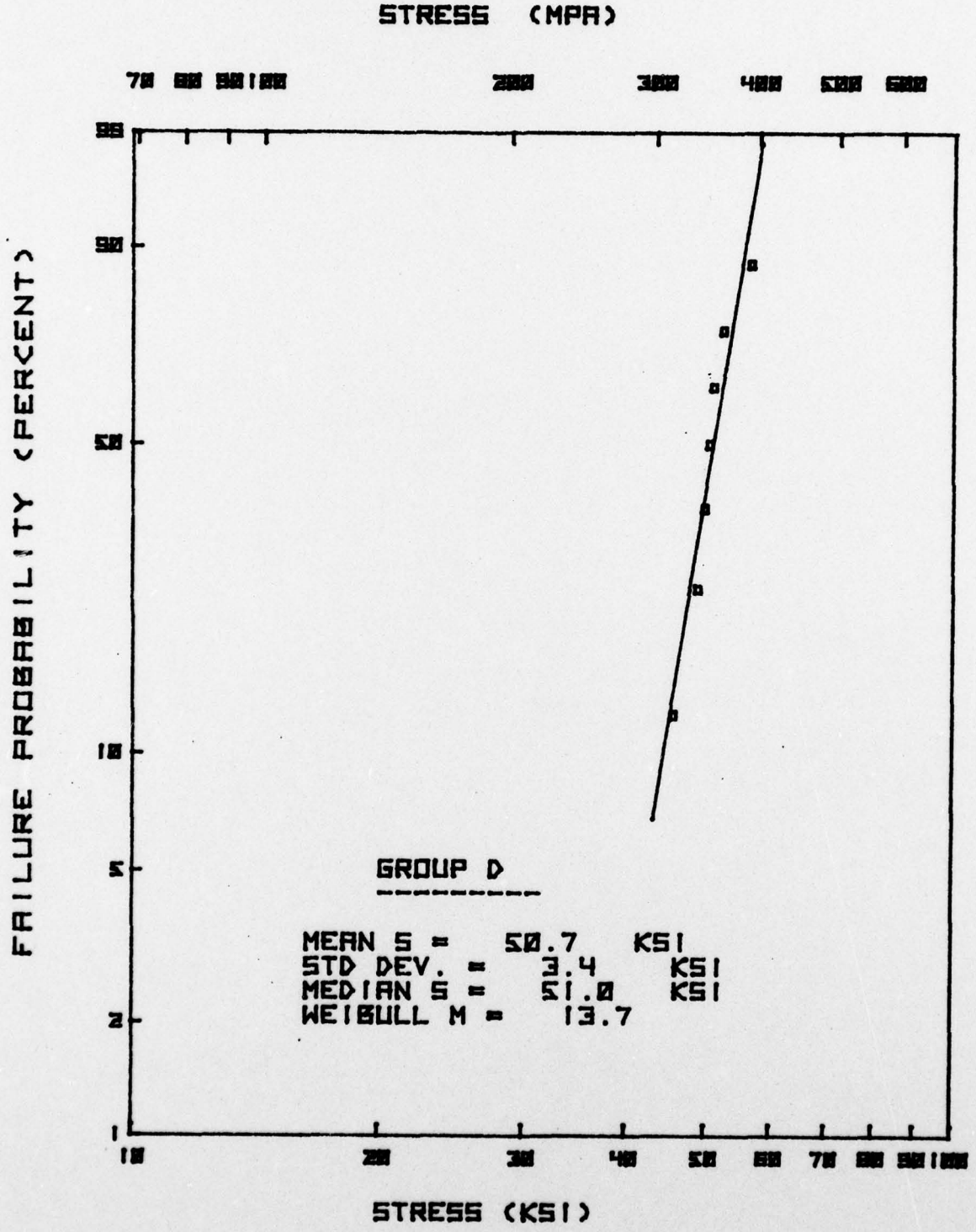
STRESS (MPA)
FAILURE PROBABILITY (PERCENT)
GROUP D
MEAN S = 50.7 KSI
STD DEV. = 3.4 KSI
MEDIAN S = 51.0 KSI
WEIBULL M = 13.7
STRESS (KSI)

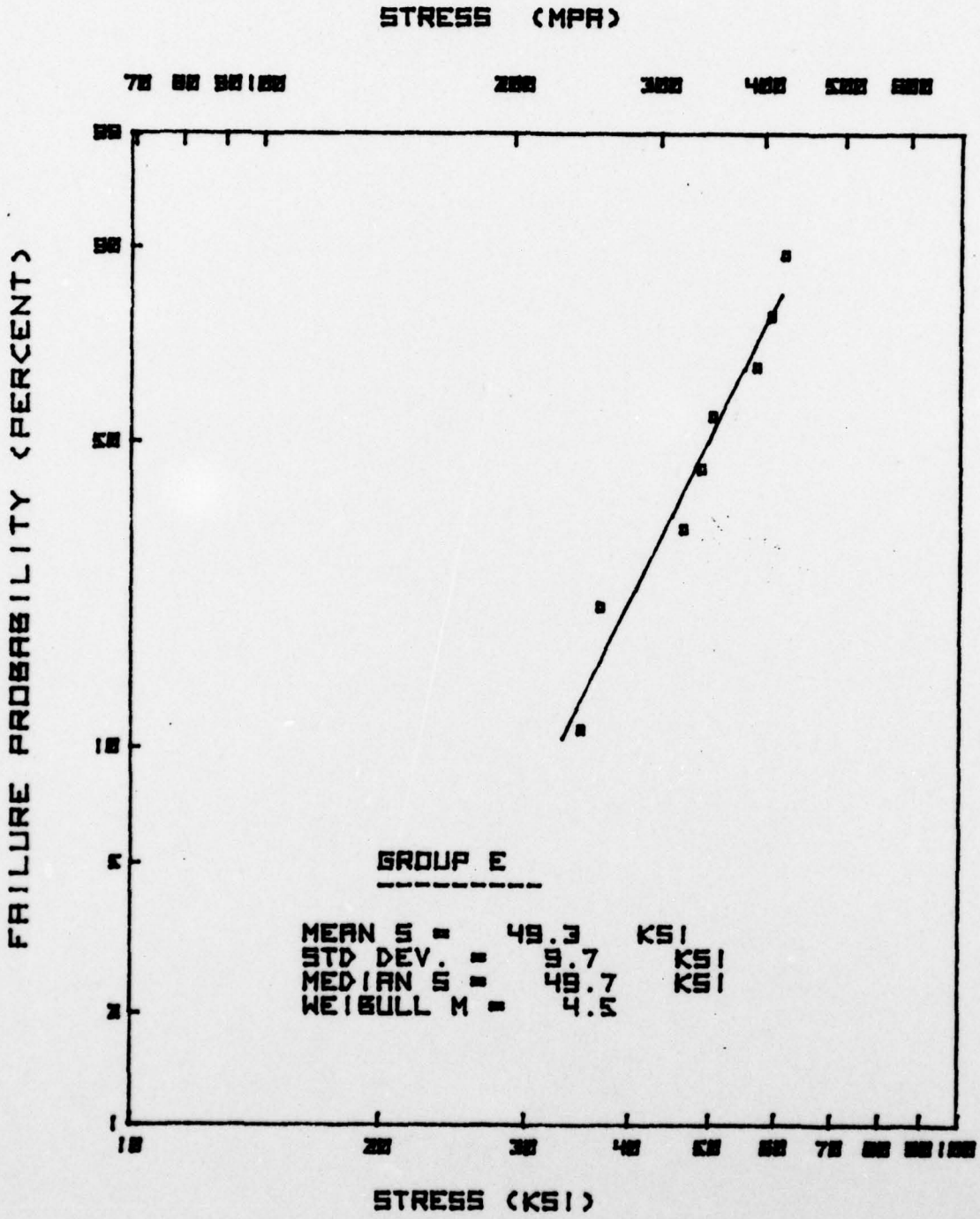
STRESS (MPA)
FAILURE PROBABILITY (PERCENT)
GROUP E
MEAN S = 49.3 KSI
STD DEV. = 9.7 KSI
MEDIAN S = 49.7 KSI
WEIBULL M = 4.5
STRESS (KSI)

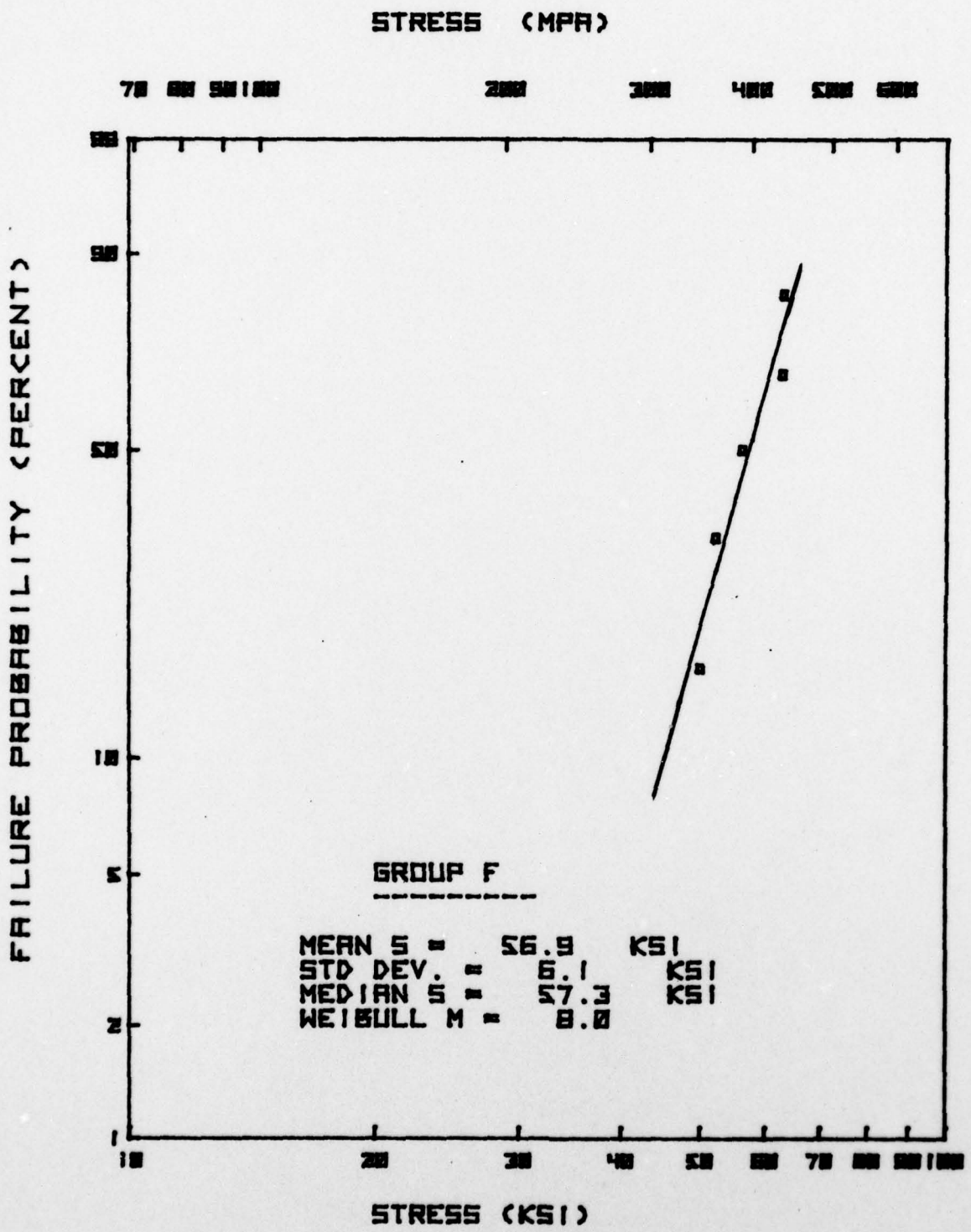
STRESS (MPA)
FAILURE PROBABILITY (PERCENT)
STRESS (KSI)
GROUP F
MEAN S = 56.9 KSI
STD DEV. = 6.1 KSI
MEDIAN S = 57.3 KSI
WEIBULL M = 8.0

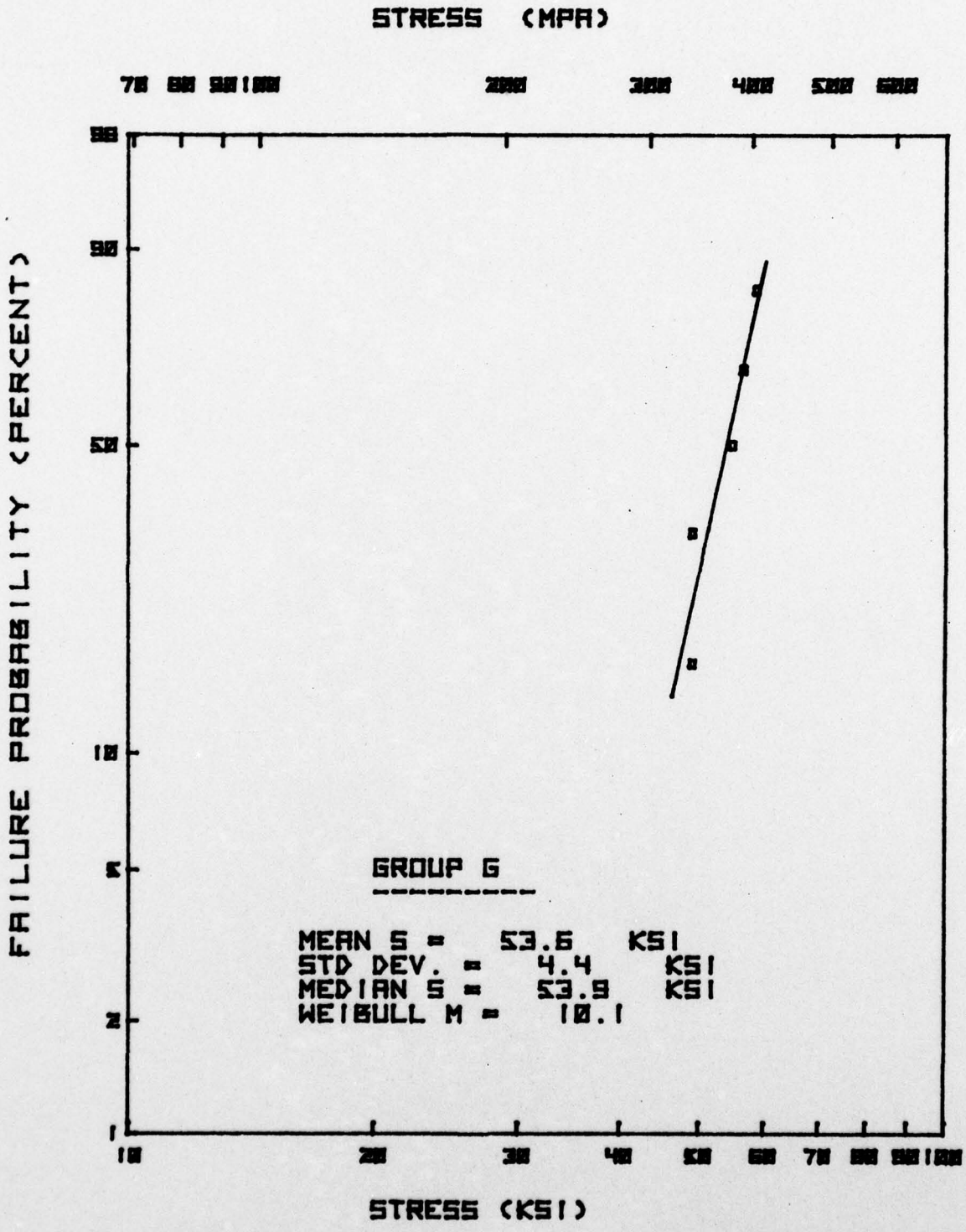
STRESS (MPA)
FAILURE PROBABILITY (PERCENT)
GROUP G
MEAN S = 53.6 KSI
STD DEV. = 4.4 KSI
MEDIAN S = 53.9 KSI
WEIBULL M = 10.1
STRESS (KSI)

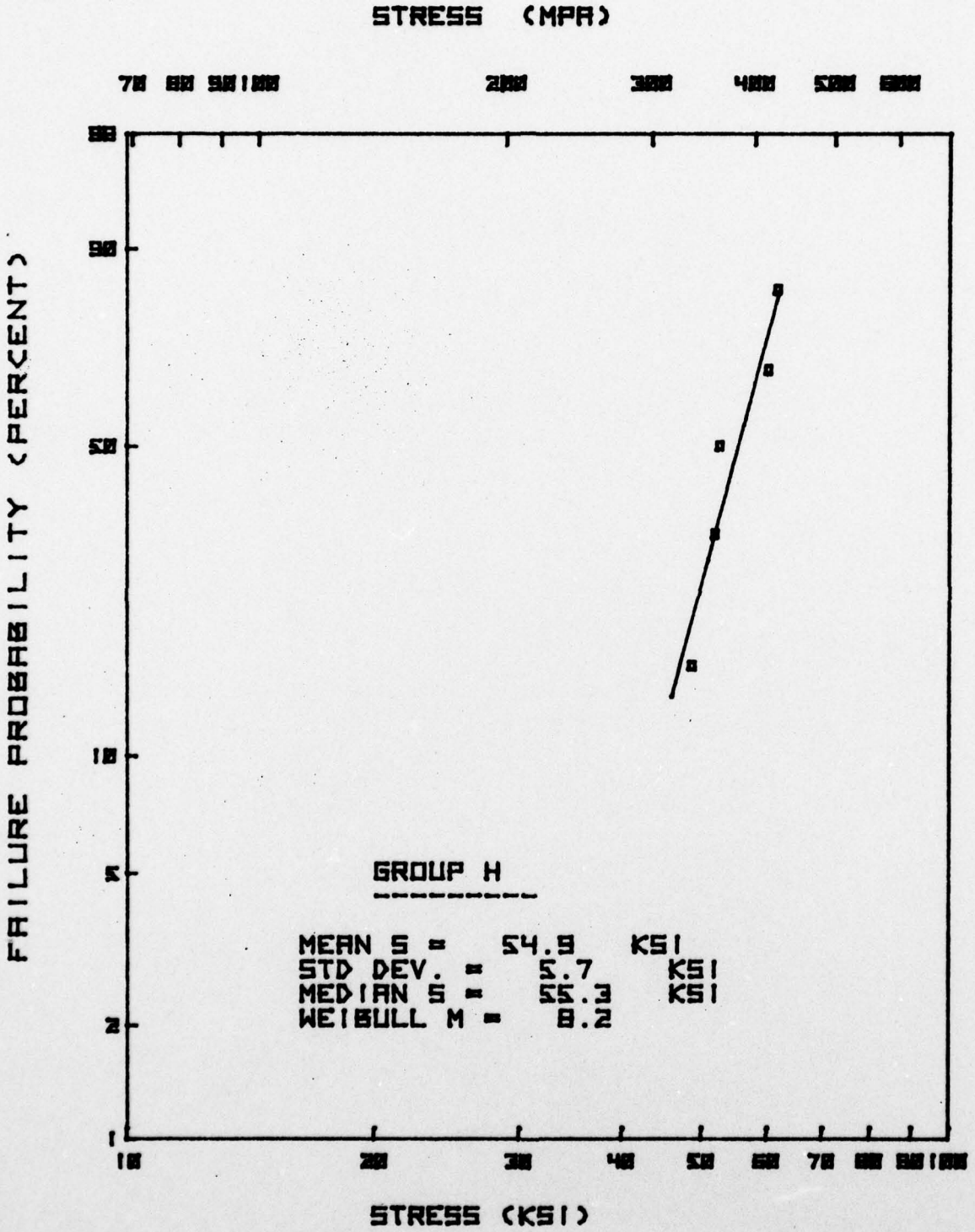
STRESS (MPA)
FAILURE PROBABILITY (PERCENT)
GROUP H
MEAN S = 54.9 KSI
STD DEV. = 5.7 KSI
MEDIAN S = 55.3 KSI
WEIBULL M = 8.2
STRESS (KSI)

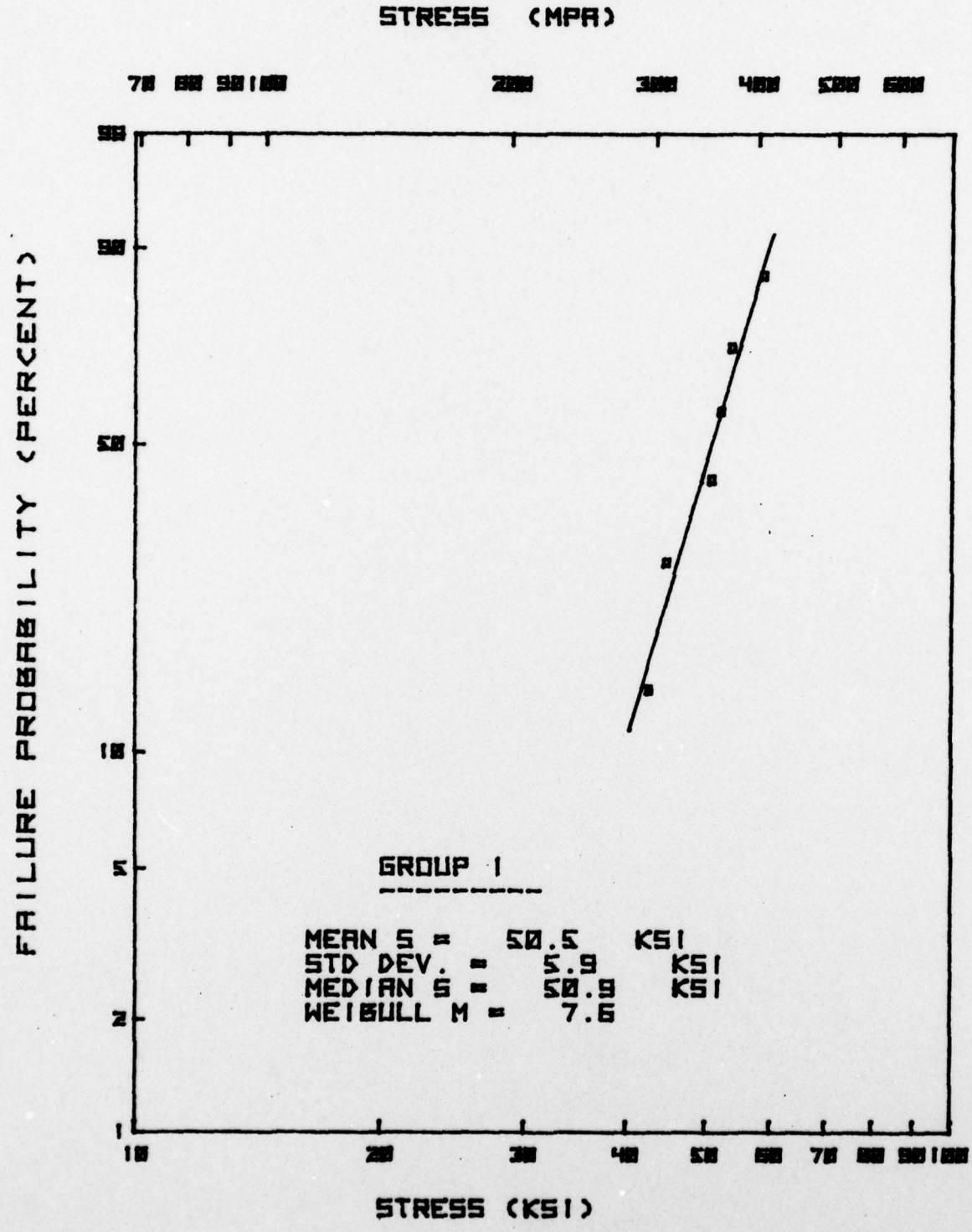
STRESS (MPA)
FAILURE PROBABILITY (PERCENT)
GROUP 1
MEAN S = 50.5 KSI
STD DEV. = 5.9 KSI
MEDIAN S = 50.9 KSI
WEIBULL M = 7.6
STRESS (KSI)

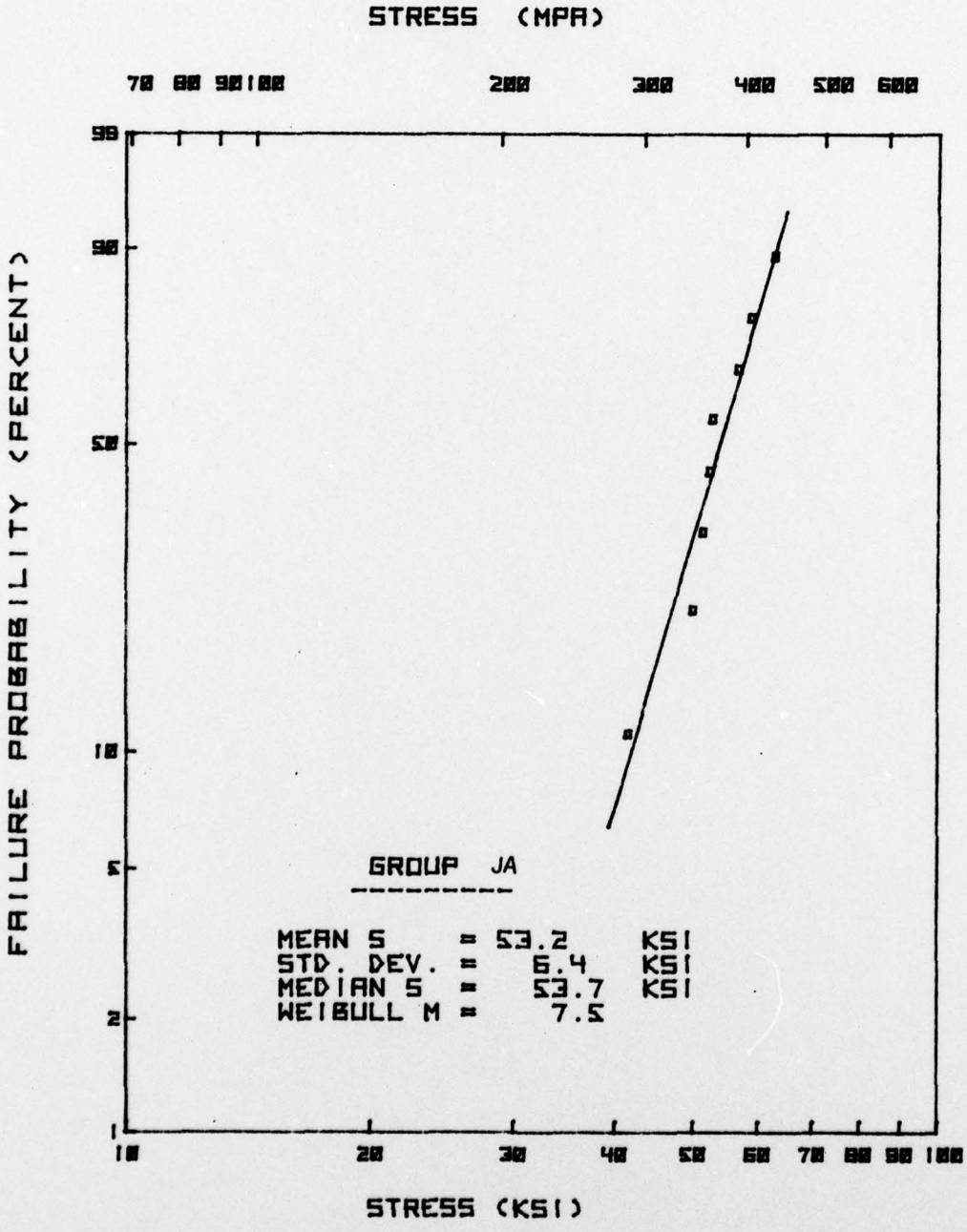
STRESS (MPA)
70 80 90 100 200 300 400 500 600
99
90
50
10
5
2
1
FAILURE PROBABILITY (PERCENT)
GROUP JA
MEAN S = 53.2 KSI
STD. DEV. = 6.4 KSI
MEDIAN S = 53.7 KSI
WEIBULL M = 7.5
10 20 30 40 50 60 70 80 90 100
STRESS (KSI)

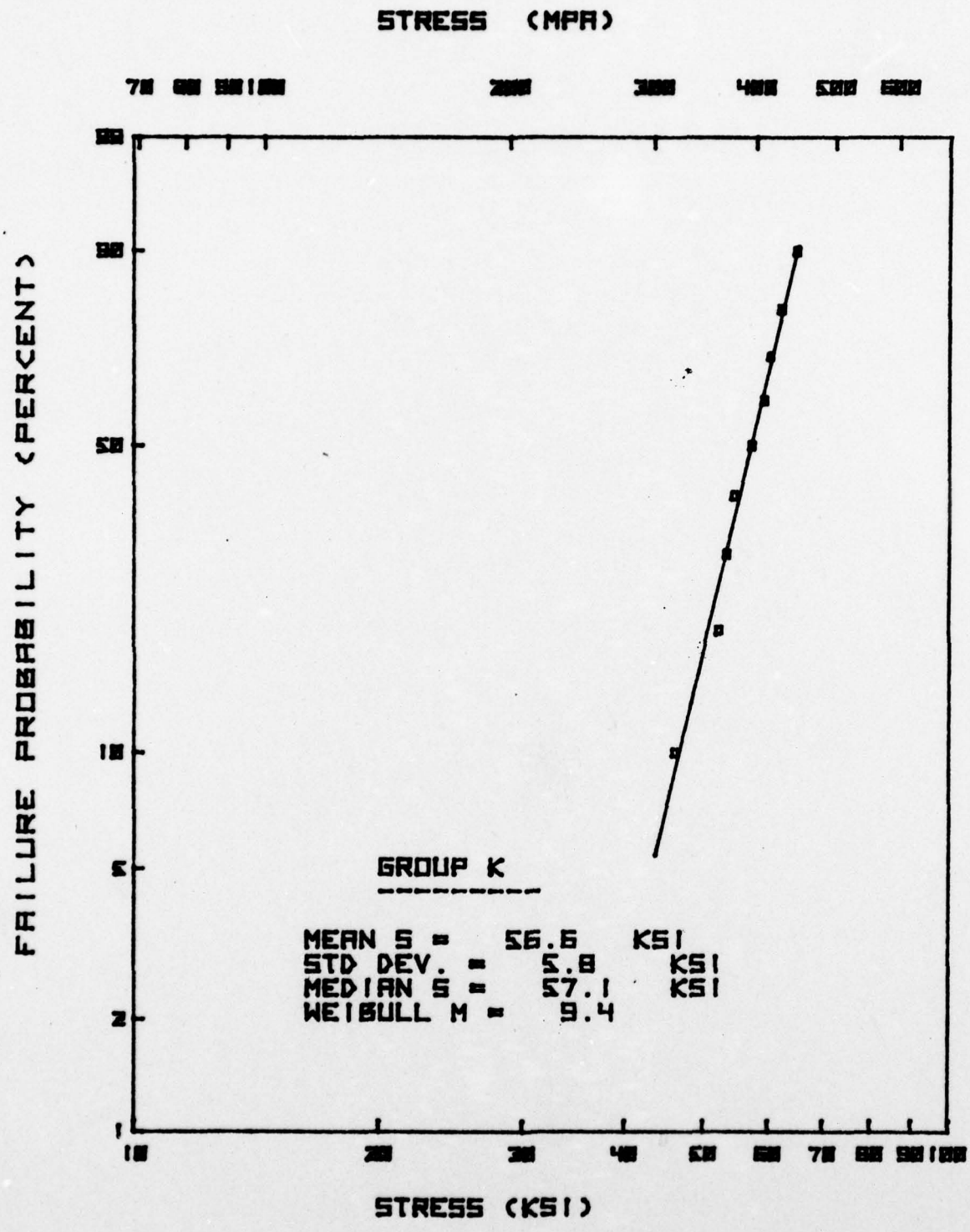
STRESS (MPA)
FAILURE PROBABILITY (PERCENT)
GROUP K
MEAN S = 56.6 KSI
STD DEV. = 5.8 KSI
MEDIAN S = 57.1 KSI
WEIBULL M = 9.4
STRESS (KSI)

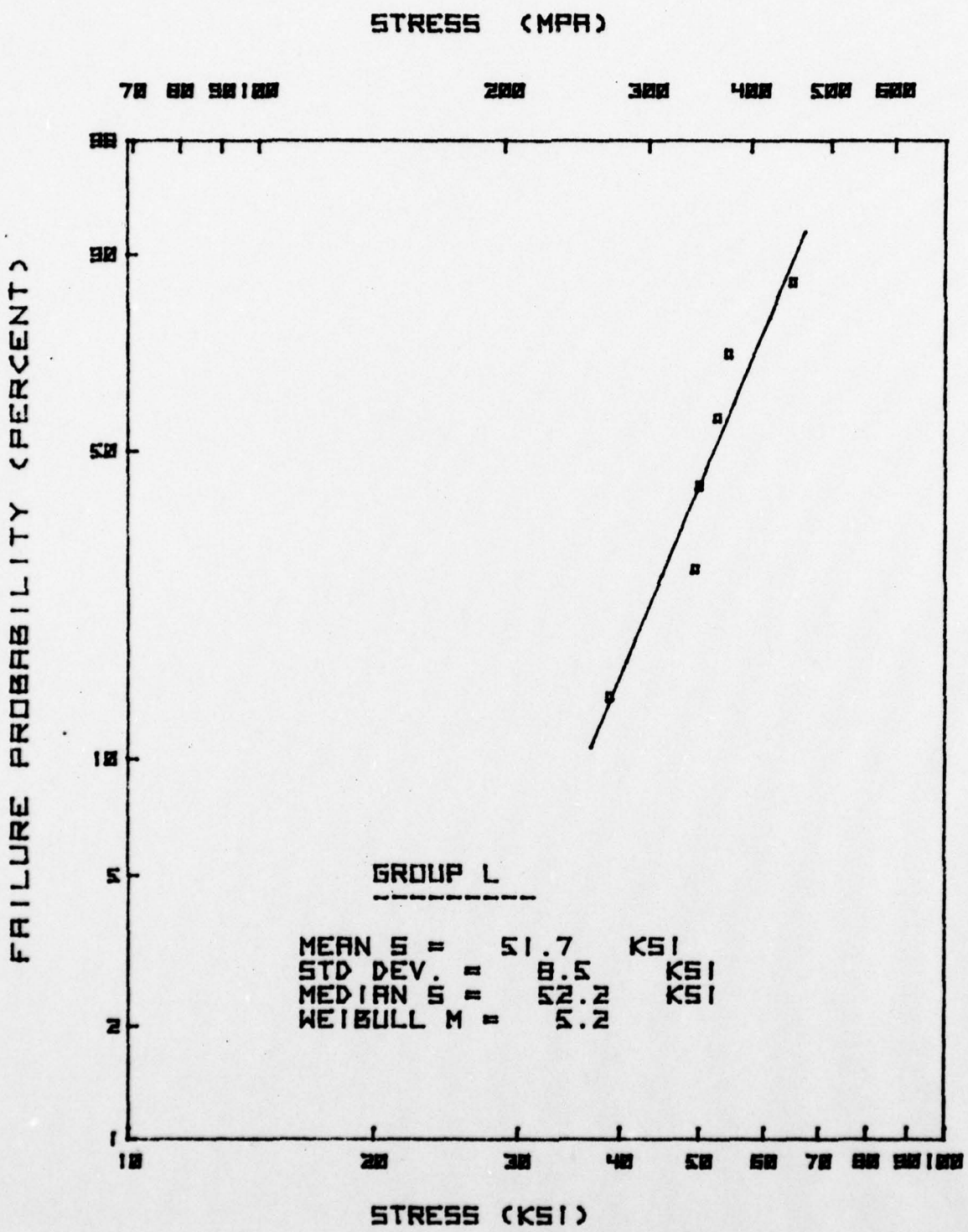
STRESS (MPA)
70 80 90 100 200 300 400 500 600
99
90
50
10
5
2
1
FAILURE PROBABILITY (PERCENT)
GROUP L
MEAN S = 51.7 KSI
STD DEV. = 8.5 KSI
MEDIAN S = 52.2 KSI
WEIBULL M = 5.2
10 20 30 40 50 60 70 80 90 100
STRESS (KSI)

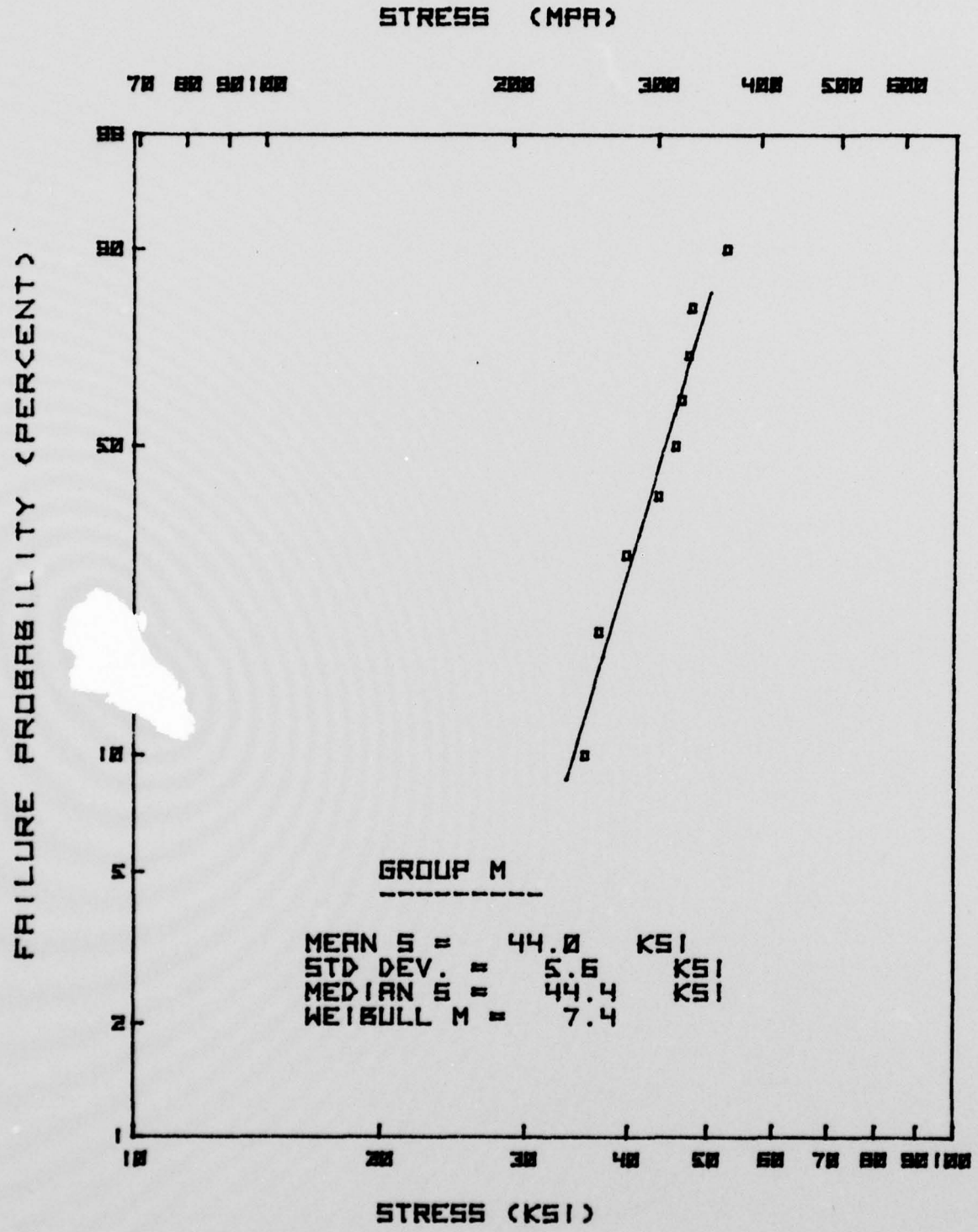
STRESS (MPA)
70 80 90 100
200
300
400
500
600
FAILURE PROBABILITY (PERCENT)
99
90
50
10
5
2
1
GROUP M
MEAN S = 44.0 KSI
STD DEV. = 5.6 KSI
MEDIAN S = 44.4 KSI
WEIBULL M = 7.4
10
20
30
40
50
60
70
80
90
100
STRESS (KSI)

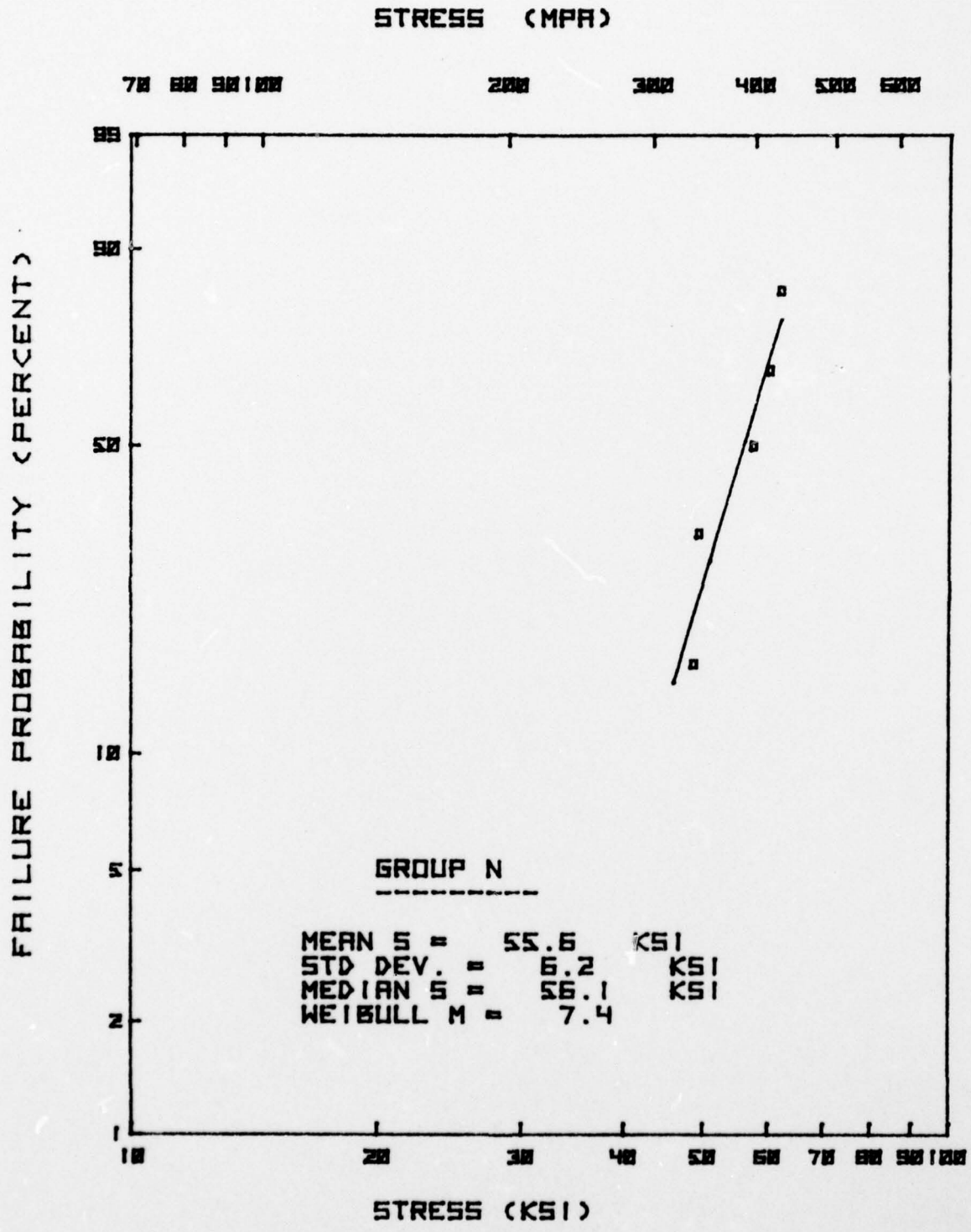
STRESS (MPA)
70 80 90 100
200
300
400
500
600
99
90
50
10
5
2
1
FAILURE PROBABILITY (PERCENT)
GROUP N
MEAN S = 55.6 KSI
STD DEV. = 6.2 KSI
MEDIAN S = 56.1 KSI
WEIBULL M = 7.4
10
20
30
40
50
60
70
80
90
100
STRESS (KSI)

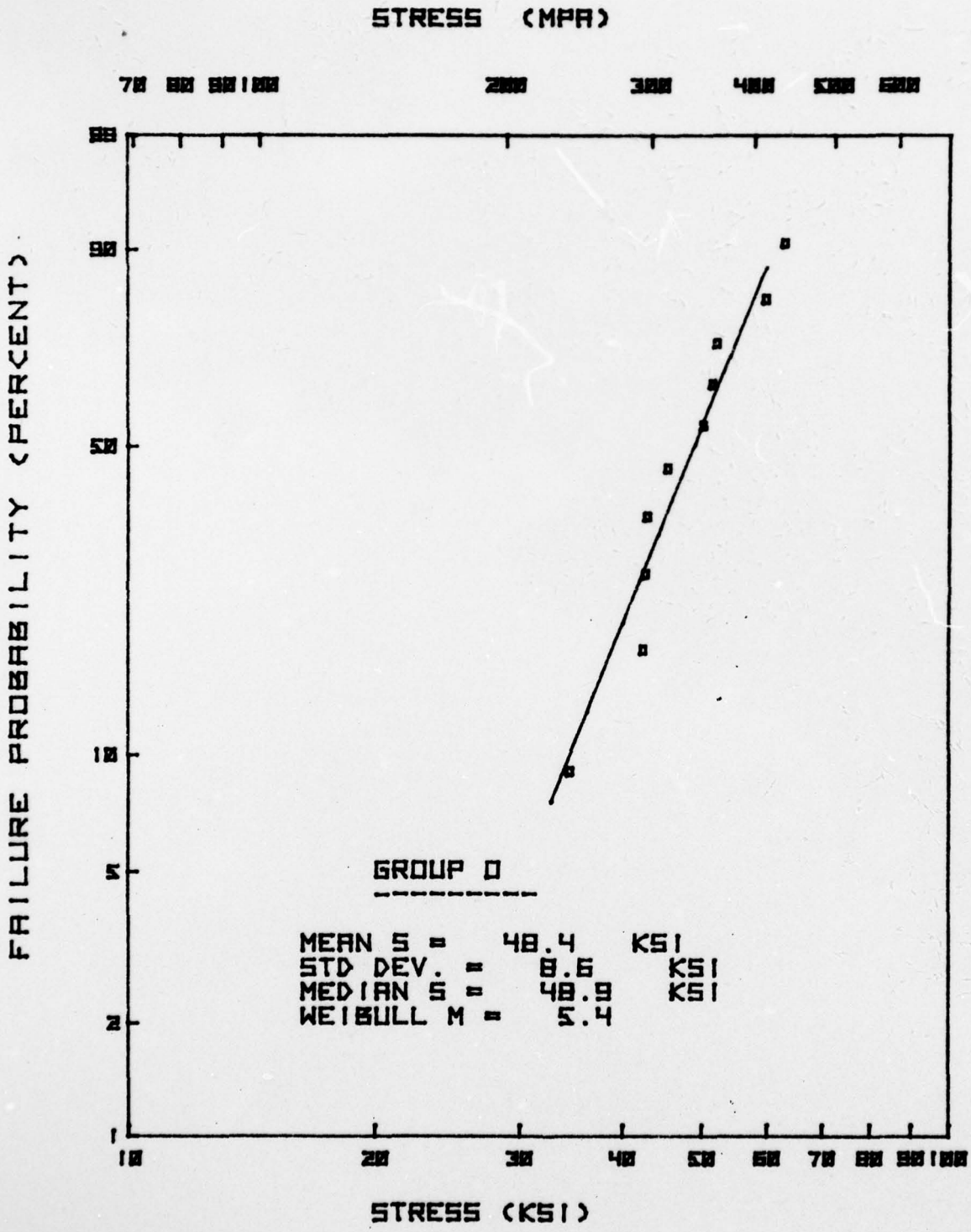
STRESS (MPA)
70 80 90 100
200
300
400
500
600
99
90
50
10
5
2
1
FAILURE PROBABILITY (PERCENT)
GROUP 0
MEAN S = 48.4 KSI
STD DEV. = 8.6 KSI
MEDIAN S = 48.9 KSI
WEIBULL M = 5.4
10
20
30
40
50
60
70
80
90
100
STRESS (KSI)

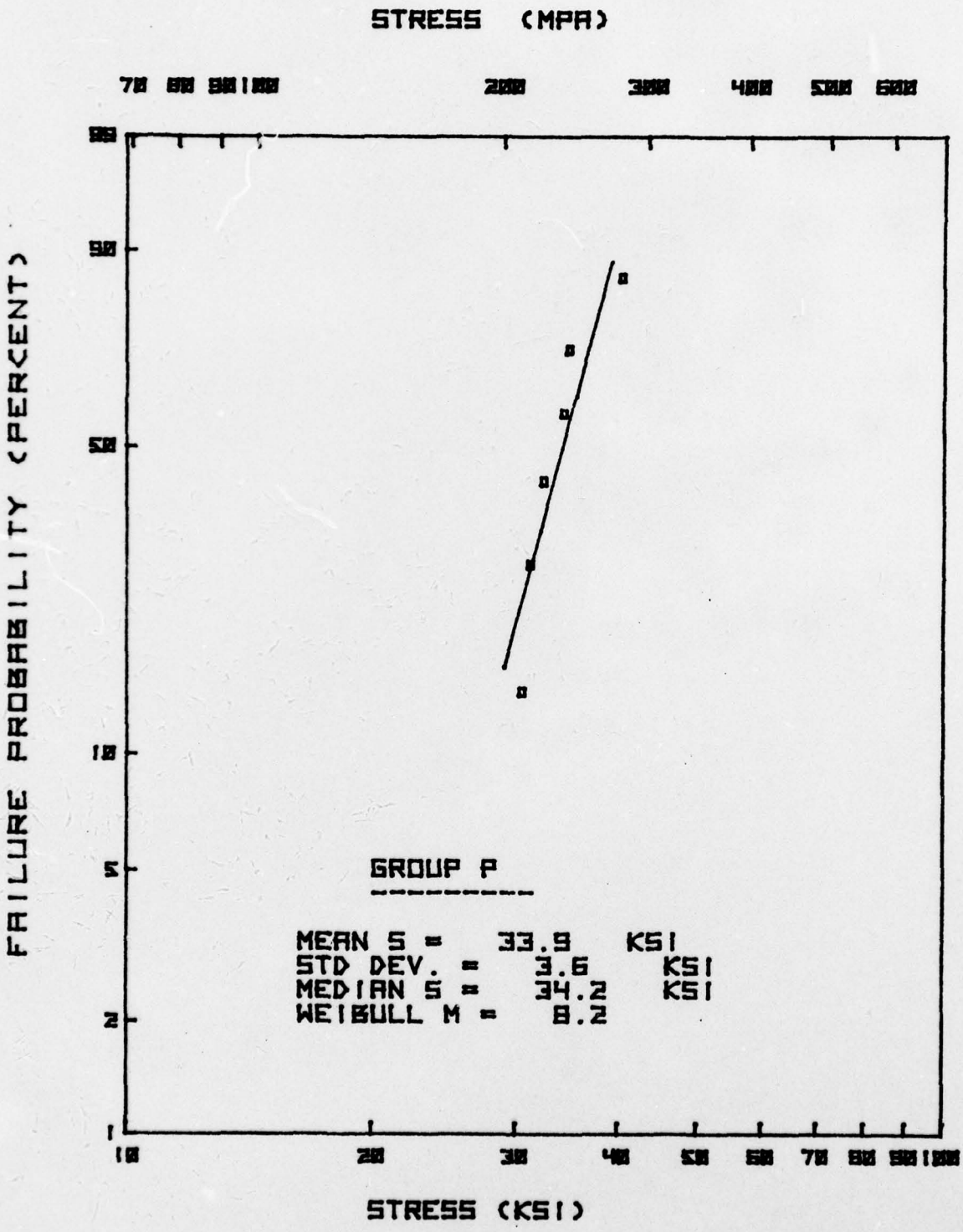
STRESS (MPA)
2000
3000
4000
5000
6000
FAILURE PROBABILITY (PERCENT)
90
50
10
5
2
1
GROUP P
MEAN S = 33.9 KSI
STD DEV. = 3.6 KSI
MEDIAN S = 34.2 KSI
WEIBULL M = 8.2
STRESS (KSI)

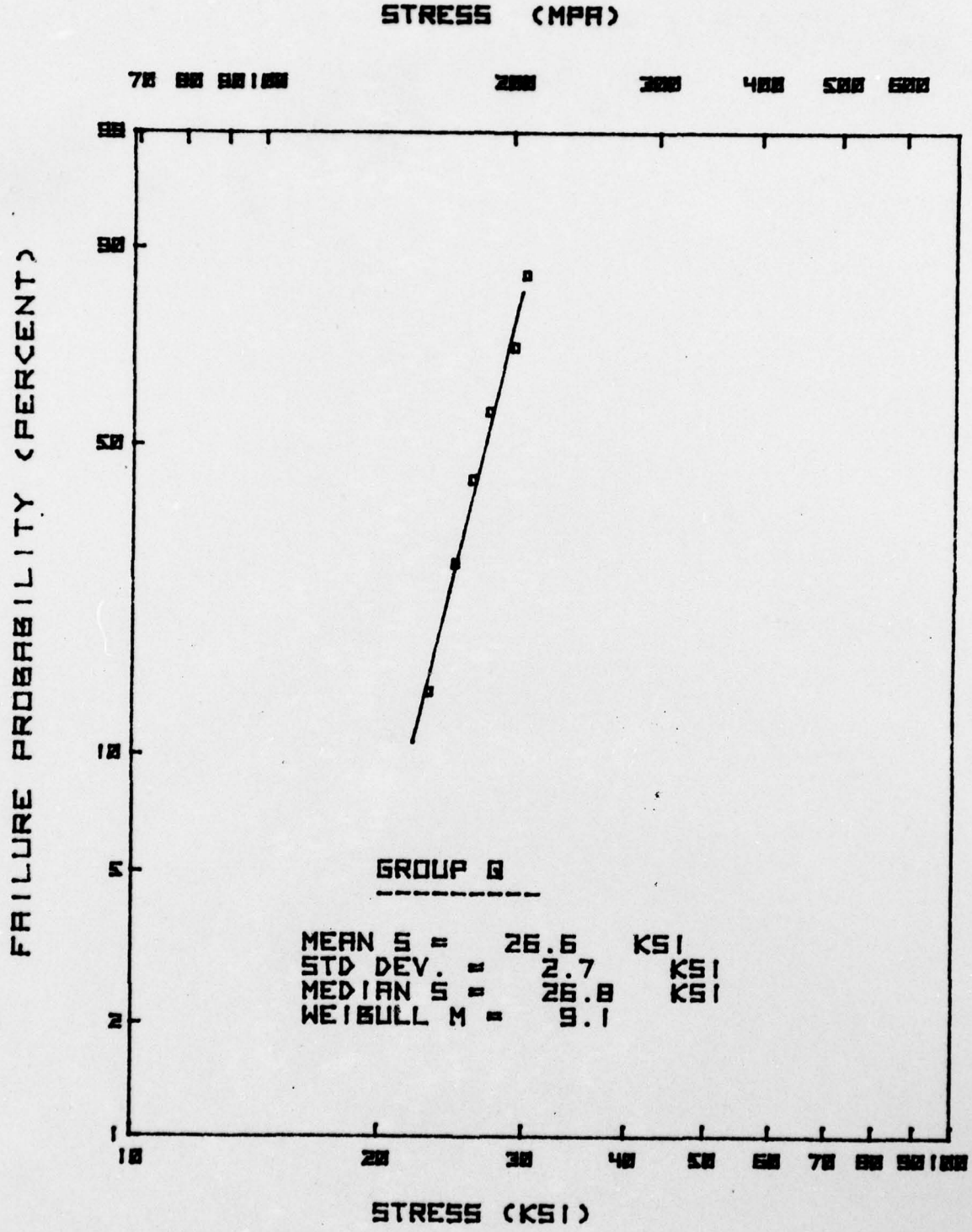
STRESS (MPA)
FAILURE PROBABILITY (PERCENT)
GROUP Q
MEAN S = 26.6 KSI
STD DEV. = 2.7 KSI
MEDIAN S = 26.8 KSI
WEIBULL M = 9.1
STRESS (KSI)

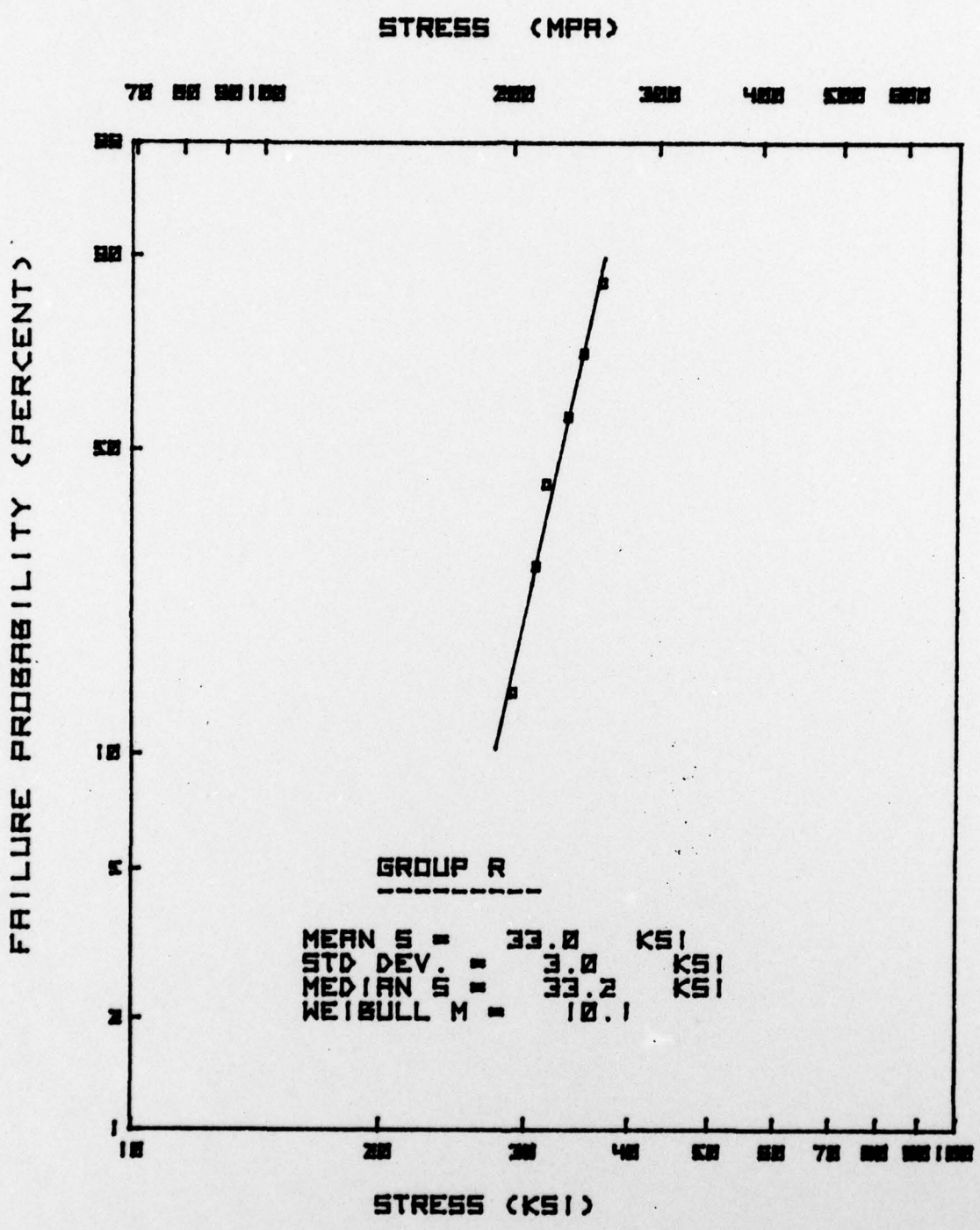
STRESS (MPA)
FAILURE PROBABILITY (PERCENT)
GROUP R
MEAN S = 33.0 KSI
STD DEV. = 3.0 KSI
MEDIAN S = 33.2 KSI
WEIBULL M = 10.1
STRESS (KSI)

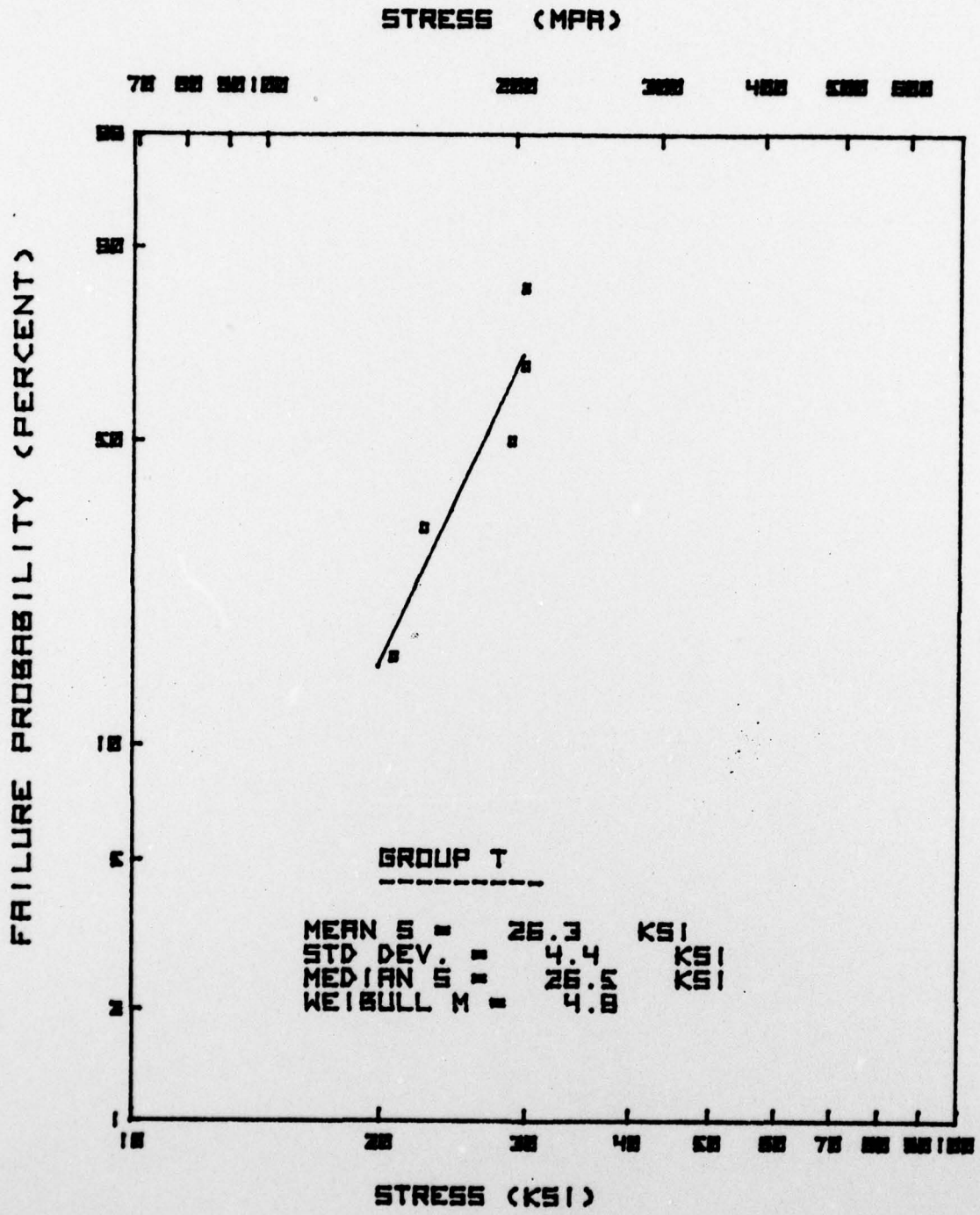
STRESS (MPA)
FAILURE PROBABILITY (PERCENT)
GROUP T
MEAN S = 26.3 KSI
STD DEV. = 4.4 KSI
MEDIAN S = 26.5 KSI
WEIBULL M = 4.8
STRESS (KSI)

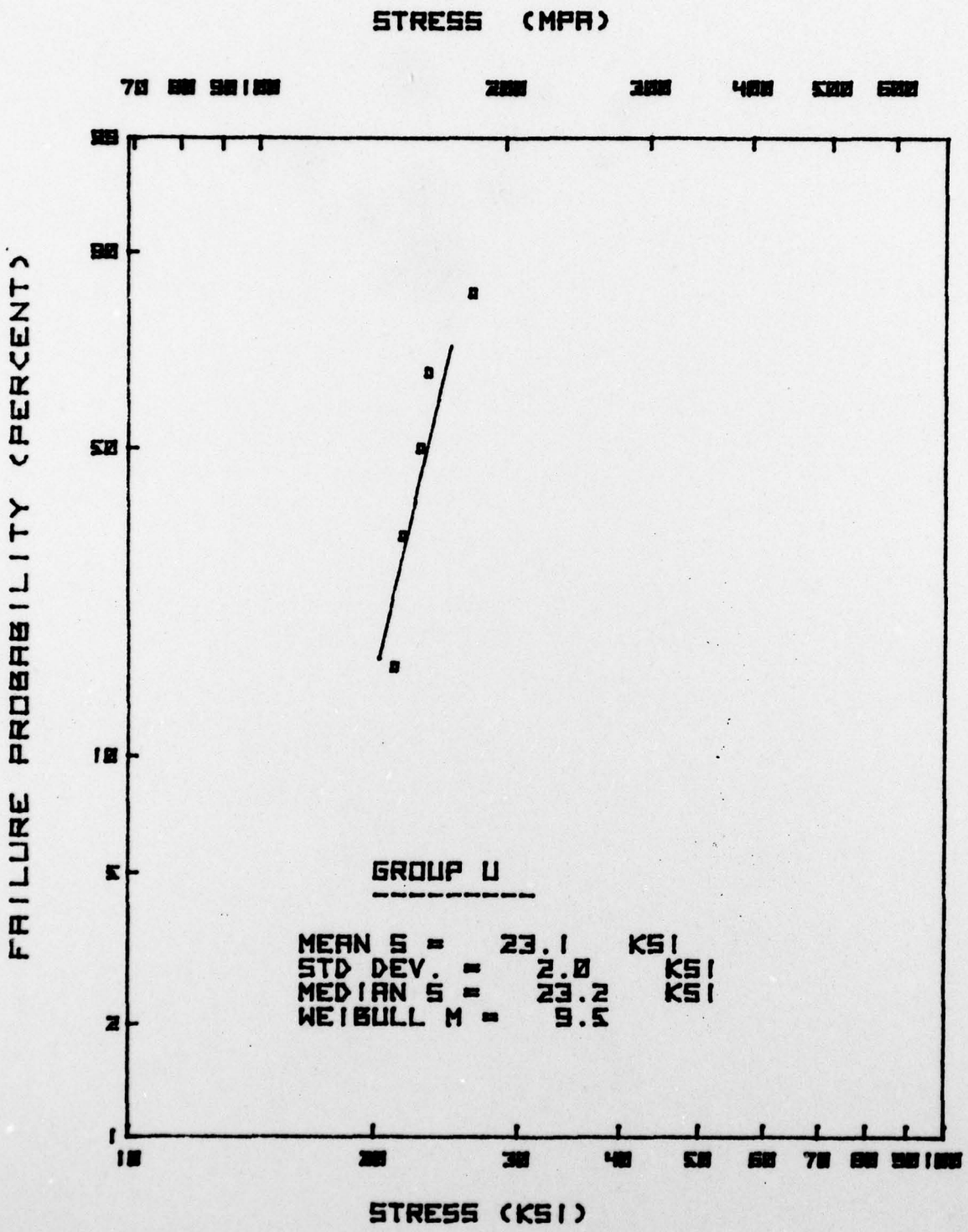
STRESS (MPA)
FAILURE PROBABILITY (PERCENT)
GROUP U
MEAN S = 23.1 KSI
STD DEV. = 2.0 KSI
MEDIAN S = 23.2 KSI
WEIBULL M = 9.5
STRESS (KSI)

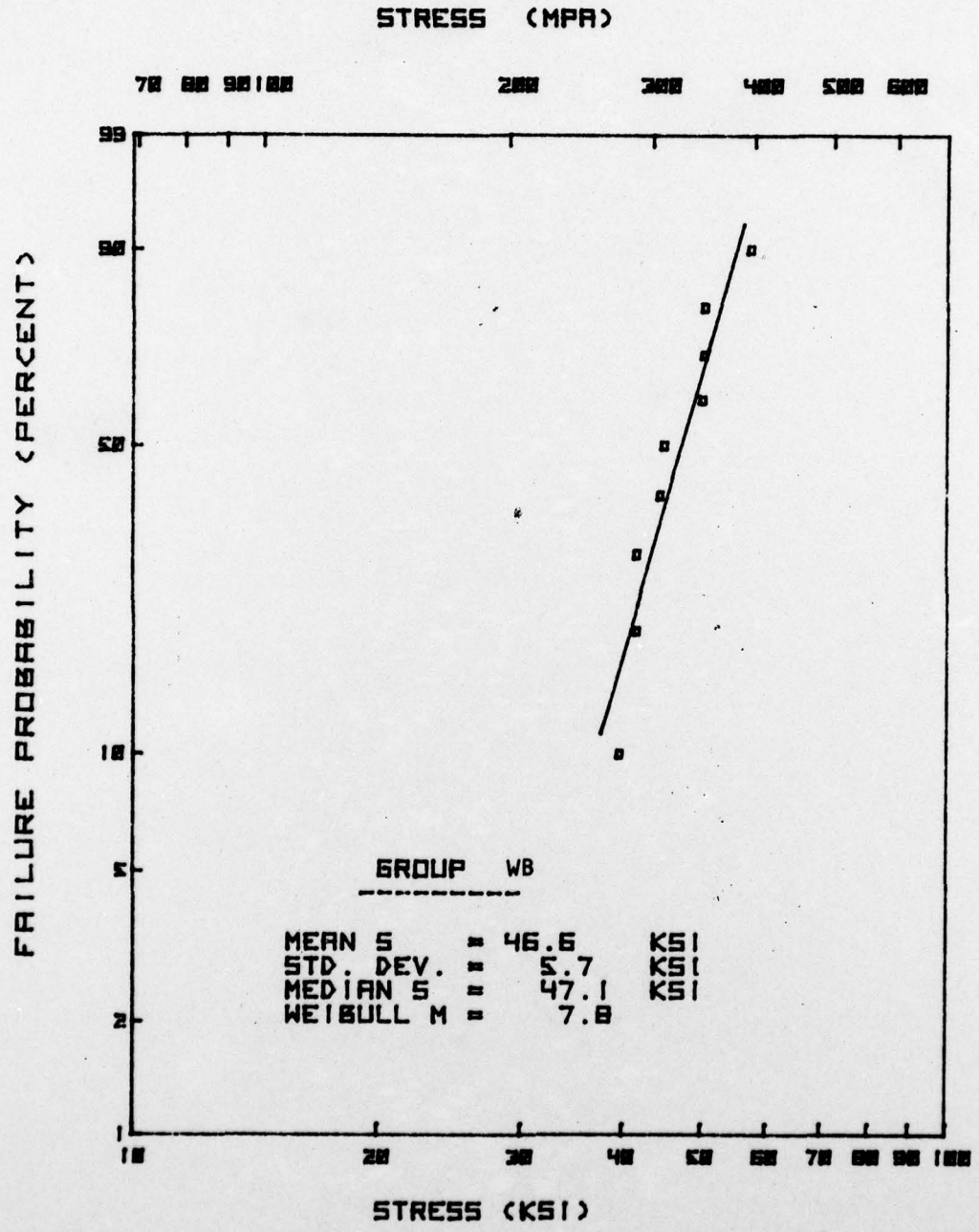
STRESS (MPA)
70 80 90 100
200
300
400
500
600
99
90
50
10
5
2
1
FAILURE PROBABILITY (PERCENT)
GROUP WB
MEAN S = 46.6 KSI
STD. DEV. = 5.7 KSI
MEDIAN S = 47.1 KSI
WEIBULL M = 7.8
10
20
30
40
50
60
70
80
90
100
STRESS (KSI)

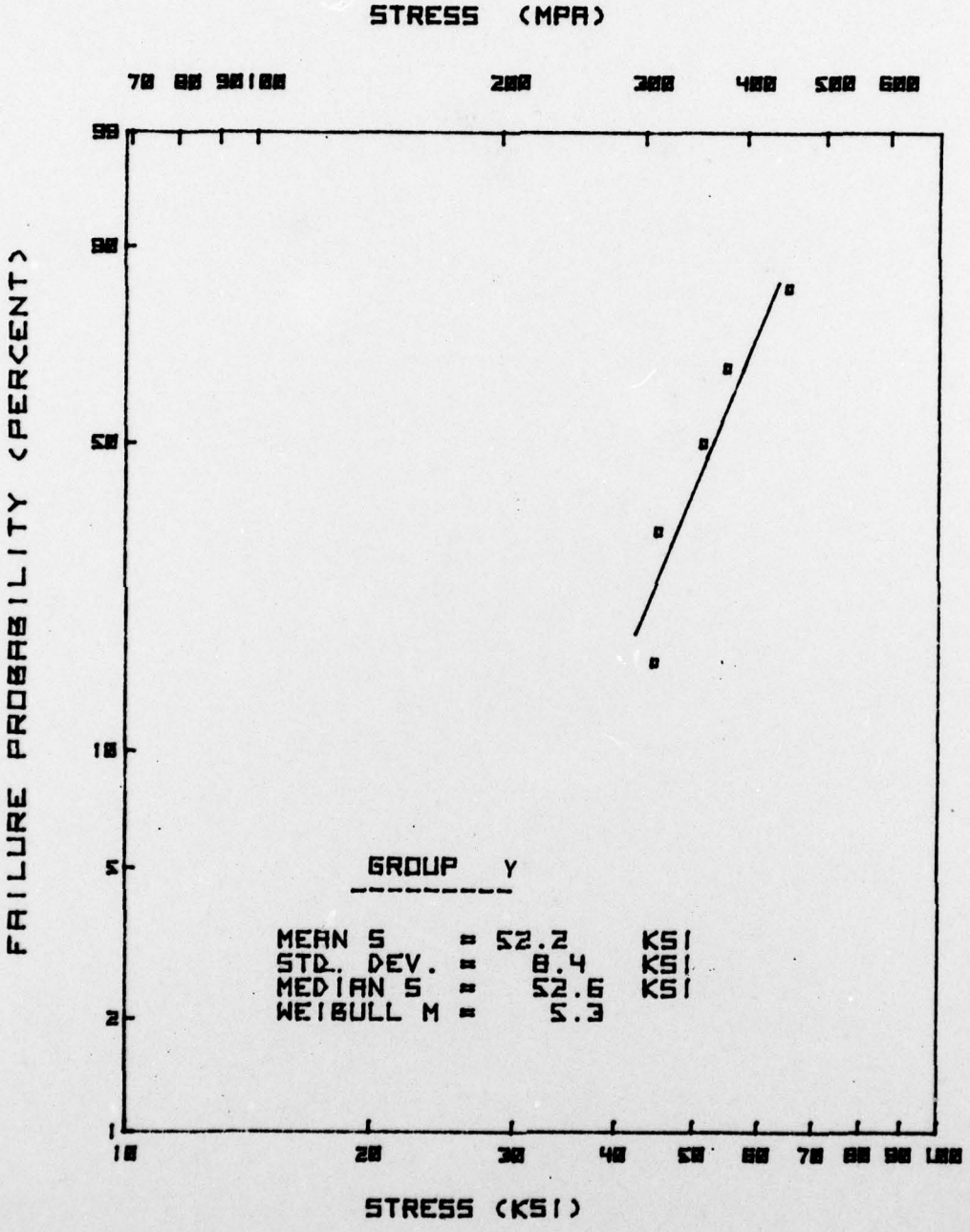
STRESS (MPA)
70 80 90 100 200 300 400 500 600
99
90
50
10
5
2
1
FAILURE PROBABILITY (PERCENT)
GROUP Y
MEAN S = 52.2 KSI
STD. DEV. = 8.4 KSI
MEDIAN S = 52.6 KSI
WEIBULL M = 5.3
10 20 30 40 50 60 70 80 90 100
STRESS (KSI)

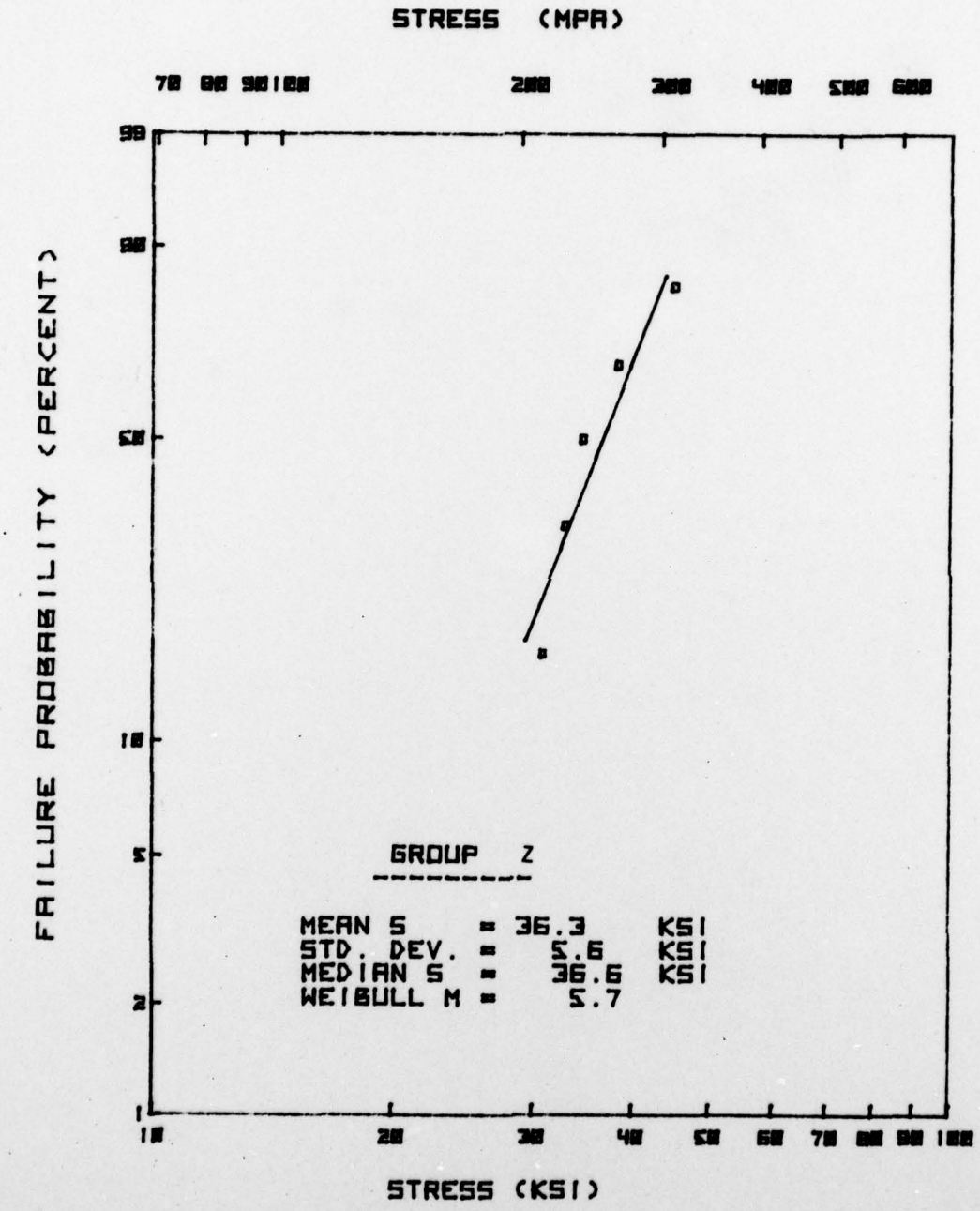
STRESS (MPA)
70 80 90 100 200 300 400 500 600
99
90
50
10
5
2
1
FAILURE PROBABILITY (PERCENT)
GROUP Z
MEAN S = 36.3 KSI
STD. DEV. = 5.6 KSI
MEDIAN S = 36.6 KSI
WEIBULL M = 5.7
10 20 30 40 50 60 70 80 90 100
STRESS (KSI)

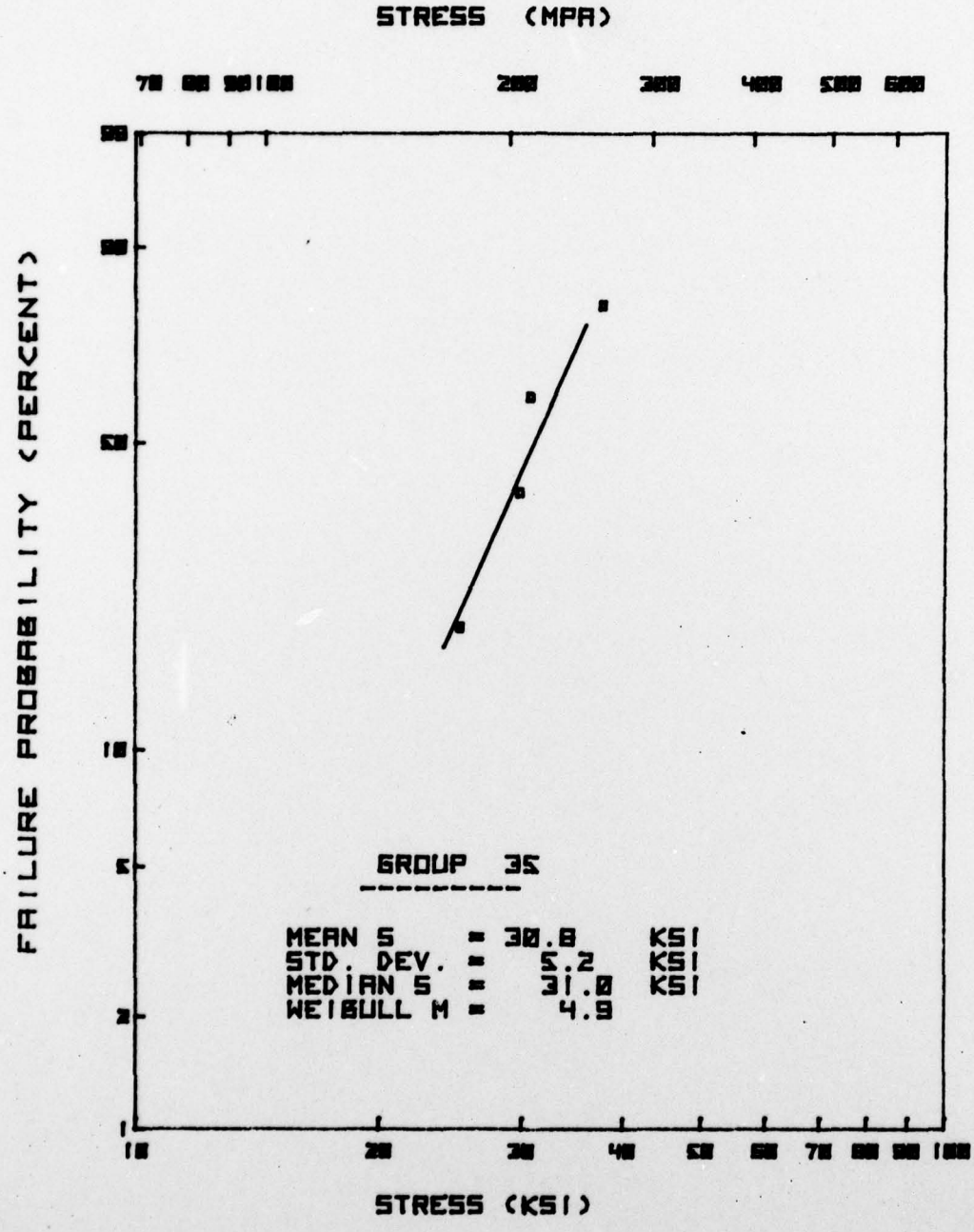
STRESS (MPA)
FAILURE PROBABILITY (PERCENT)
GROUP 35
MEAN S = 30.8 KSI
STD. DEV. = 5.2 KSI
MEDIAN S = 31.0 KSI
WEIBULL M = 4.9
STRESS (KSI)

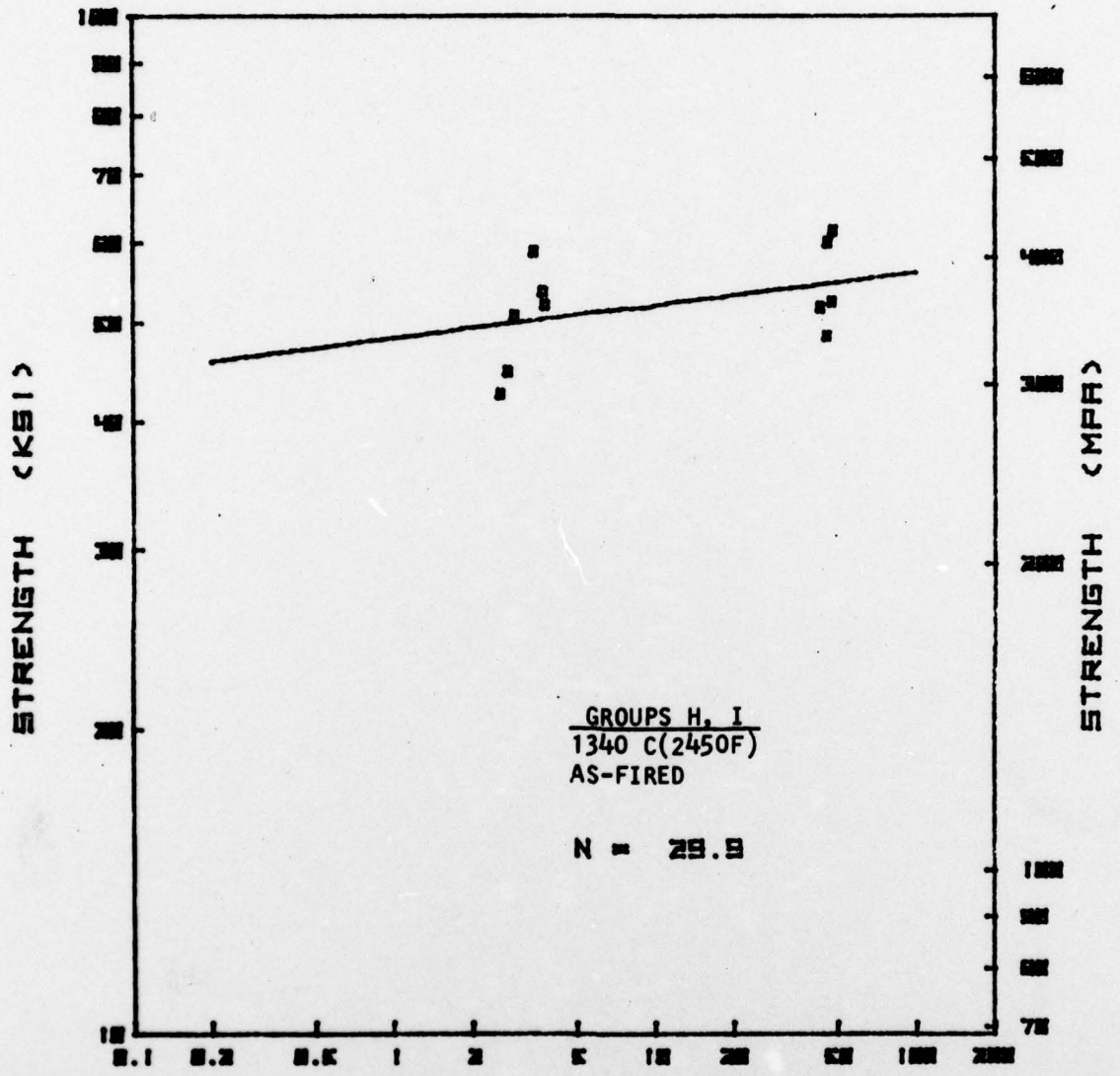
STRENGTH (KSI)
STRENGTH (MPA)
GROUPS H, I
1340 C(2450F)
AS-FIRED
N = 29.9
0.1
0.2
0.5
1
2
5
10
20
50
100
200
STRAIN RATE (MICRO IN/IN/SEC)

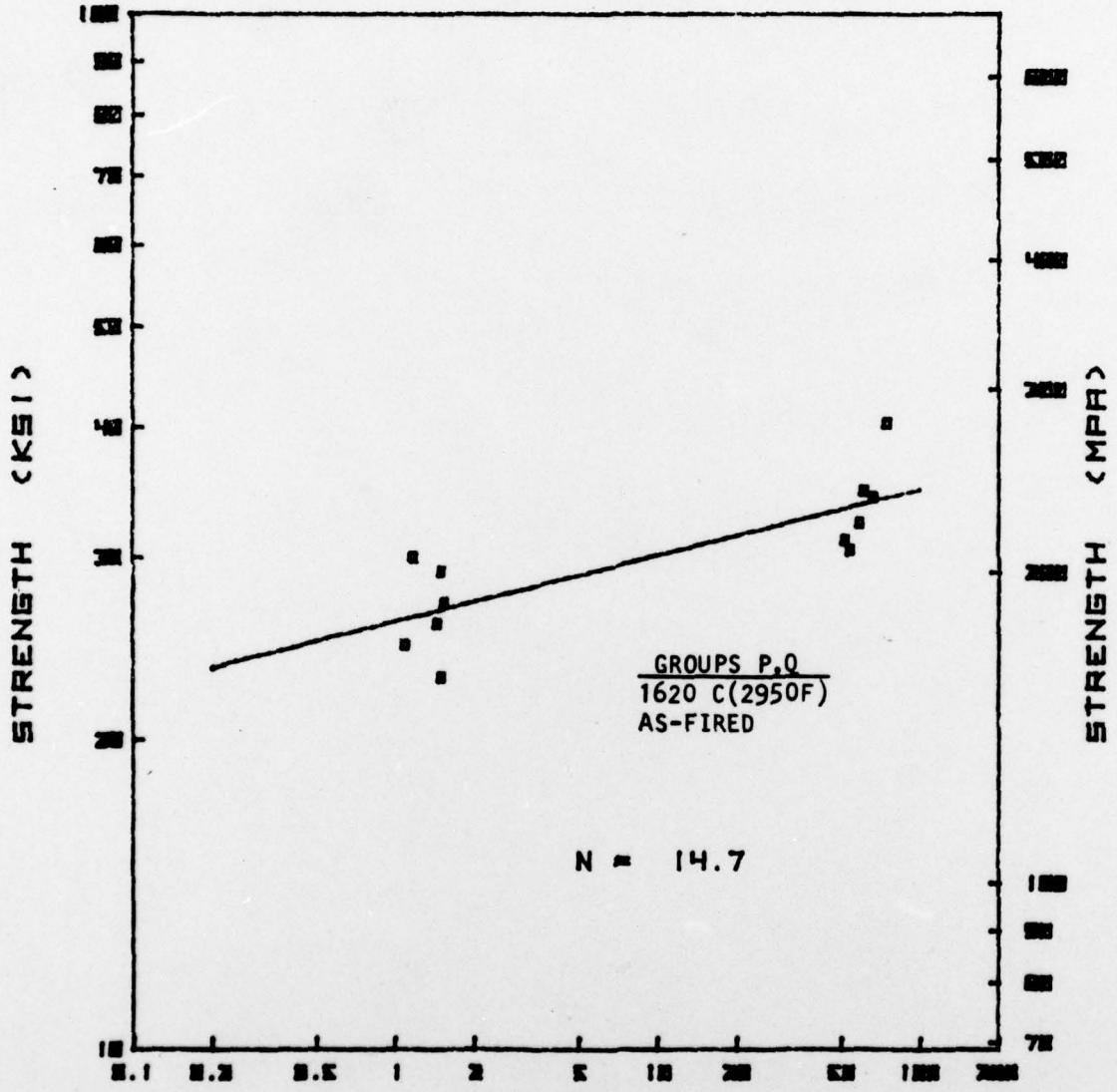
STRENGTH (KSI)
STRENGTH (MPA)
GROUPS P,Q
1620 C(2950F)
AS-FIRED
N = 14.7
STRAIN RATE (MICRO IN/IN/SEC)

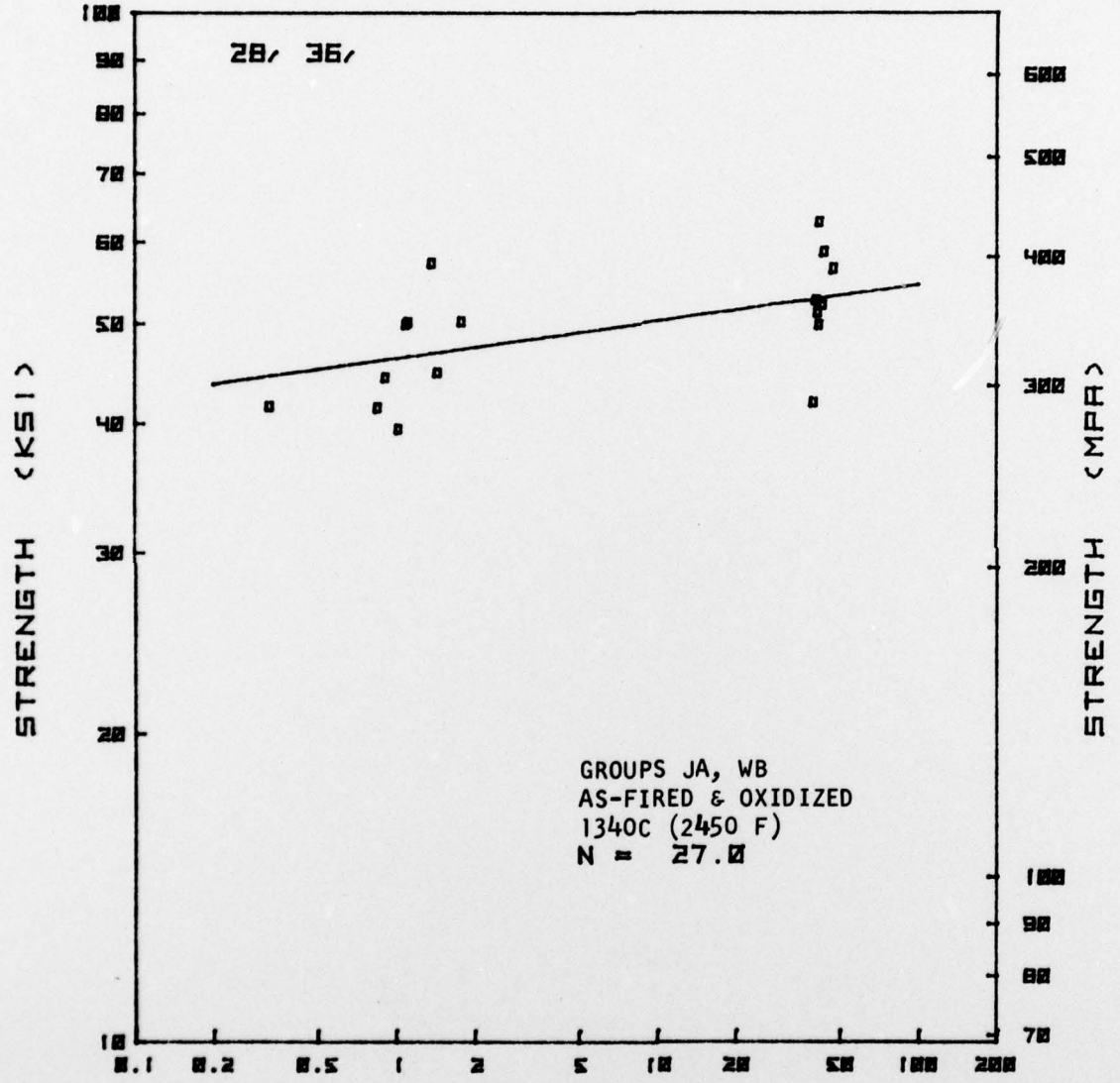
28/ 36/
GROUPS JA, WB
AS-FIRED & OXIDIZED
1340C (2450 F)
N = 27.0
STRENGTH (KSI)
STRENGTH (MPA)
STRAIN RATE (MICRO IN/IN/SEC)
100
90
80
70
60
50
40
30
20
10
600
500
400
300
200
100
90
80
70
0.1
0.2
0.5
1
2
5
10
20
50
100
200

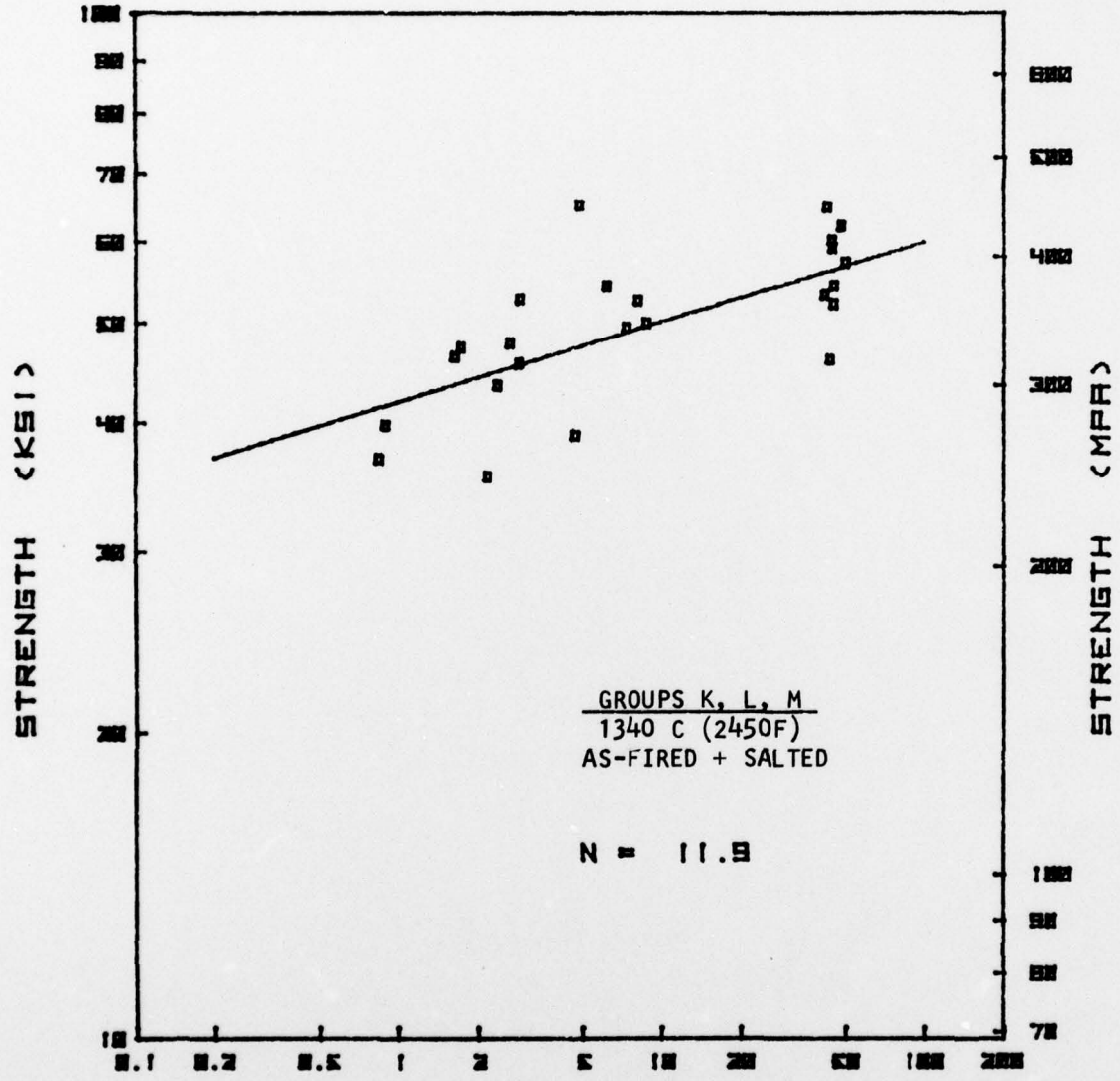
STRENGTH (KSI)
STRENGTH (MPA)
GROUPS K, L, M
1340 C (2450F)
AS-FIRED + SALTED
N = 11.9
0.1
0.2
0.5
1
2
5
10
20
50
100
200
STRAIN RATE (MICRO IN/IN/SEC)

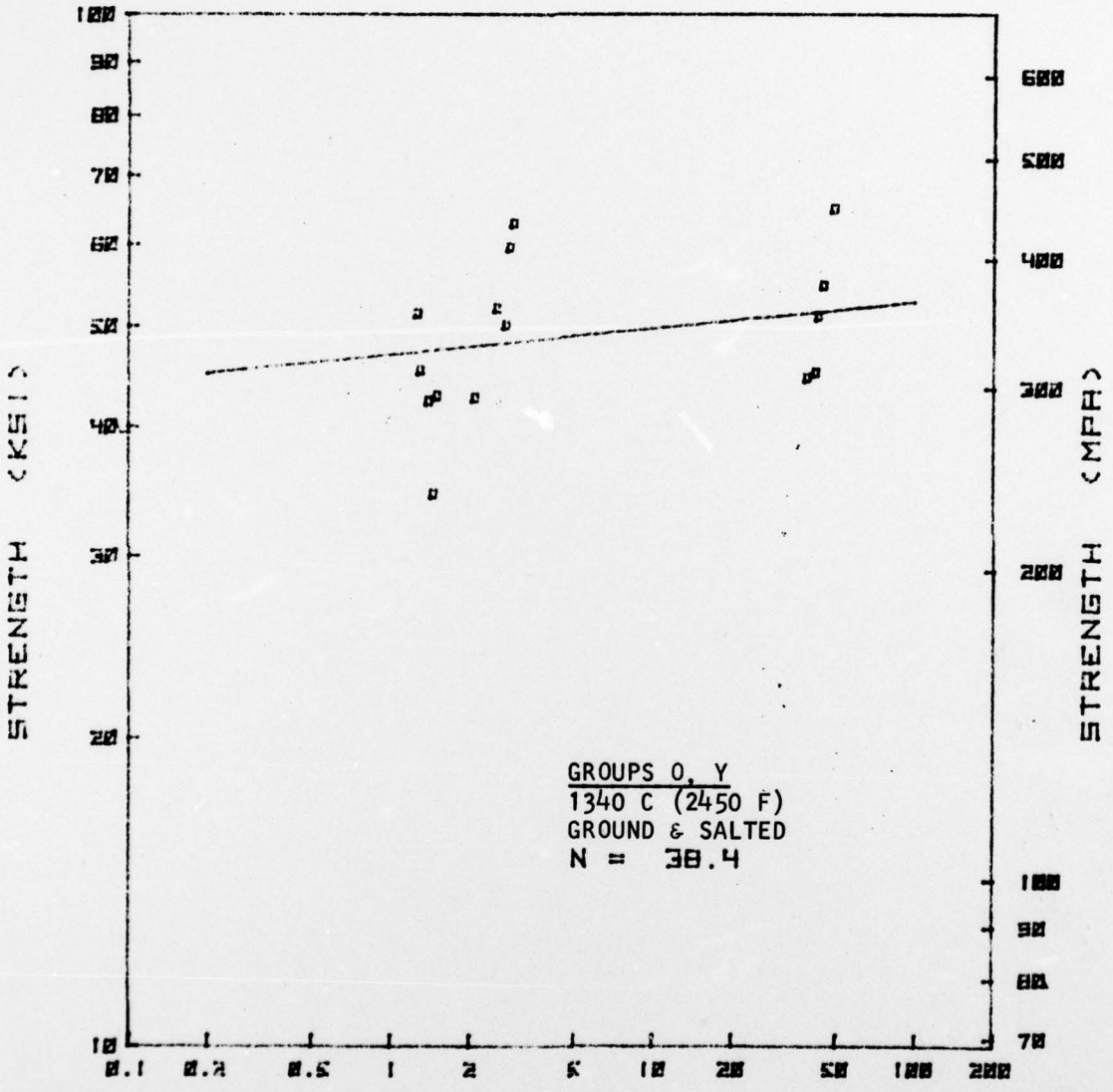
STRENGTH (KSI)
STRENGTH (MPA)
STRAIN RATE (MICRO IN/IN/SEC)
GROUPS O, Y
1340 C (2450 F)
GROUND & SALTED
N = 38.4

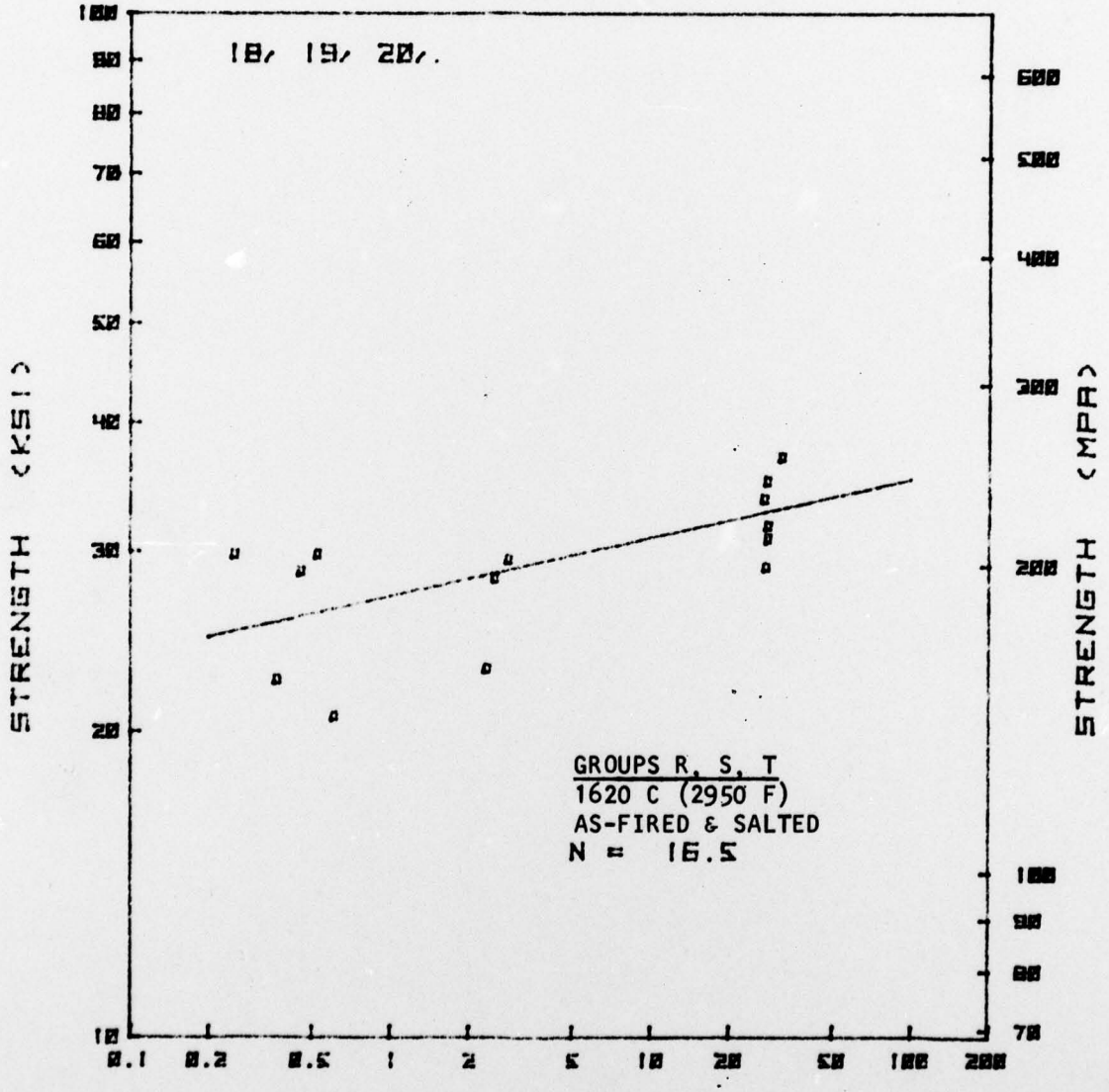
18, 19, 20.
STRENGTH (KSI)
STRENGTH (MPA)
GROUPS R, S, T
1620 C (2950 F)
AS-FIRED & SALTED
N = 16.5
0.1
0.2
0.5
1
2
5
10
20
50
100
200
STRAIN RATE (MICRO IN/IN/SEC)

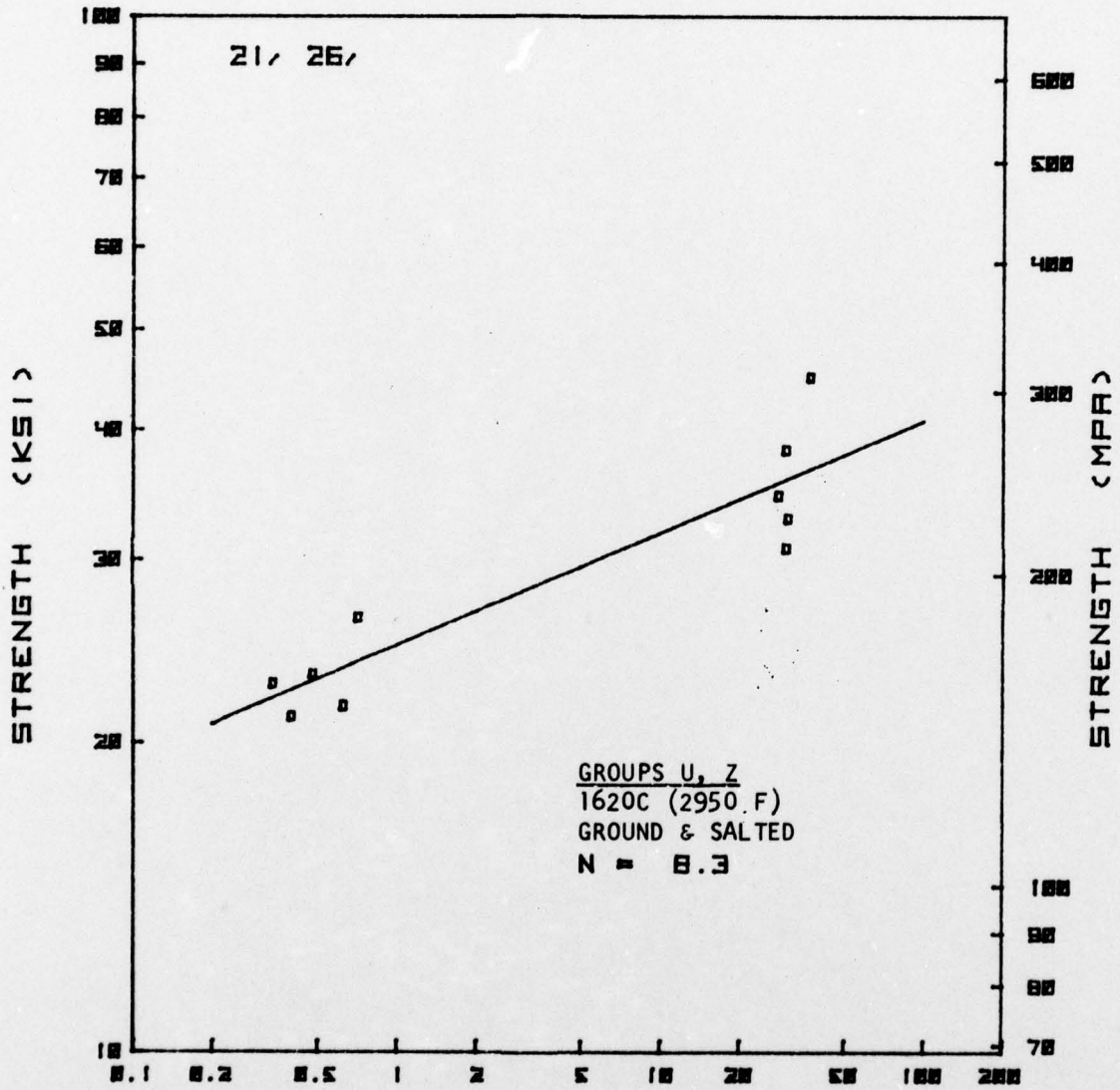
21, 26,
STRENGTH (KSI)
STRENGTH (MPA)
GROUPS U, Z
1620C (2950 F)
GROUND & SALTED
N = 8.3
STRAIN RATE (MICRO IN/IN/SEC)